

1 **Rare earth element distribution on the Fuerteventura Basal**
2 **Complex (Canary Islands, Spain): a geochemical and**
3 **mineralogical approach**

4

5 Marc Campeny¹, Inmaculada Menéndez², Luis Quevedo^{2,3}, Jorge Yepes², Ramón
6 Casillas⁴, Agustina Ahijado⁴, Jorge Méndez-Ramos³, José Mangas²

7

8 ¹ Departament de Mineralogia, Museu de Ciències Naturals de Barcelona, Passeig Picasso s/n, 08003
9 Barcelona, Spain

10 ² Instituto de Oceanografía y Cambio Global, IOCAG, Universidad de Las Palmas de Gran Canaria, 35017
11 Las Palmas de Gran Canaria, Spain

12 ³ Instituto de Materiales y Nanotecnología, Departamento de Física, Universidad de La Laguna, apartado
13 correos 456, 38200 La Laguna, Tenerife, Spain

14 ⁴ Departamento de Biología Animal, Edafología y Geología, Universidad de La Laguna, apartado correos
15 456, 38200 La Laguna, Tenerife, Spain.

16

17

18 *Correspondence to:* Marc Campeny (mcampenyc@bcn.cat)

19 **Abstract.** The Fuerteventura Basal Complex comprises of Oligocene and Miocene ultra-alkaline-
20 carbonatitic magmatic pulses with outcrops that extend across kilometre-scale areas in some specific sectors
21 of this oceanic island. Additionally, there is evidence of associated weathering materials that affect these
22 magmatic lithologies. These alkaline magmatic rocks (including trachytes, phonolites, syenites, melteigites,
23 and ijolites), carbonatites, and their associated weathering products underwent a preliminary evaluation of
24 REE contents based on mineralogical and geochemical studies. REE concentrations in carbonatites of about
25 10,300 ppm REY (REEs plus yttrium) have been detected, comparable to other locations hosting significant
26 deposits of these critical elements worldwide. Conversely, alkaline magmatic rocks and the resulting
27 weathering products display limited REE contents. Notably, REEs in carbonatites are associated with
28 primary accessory phases such as REE-bearing pyrochlore and britholite, and secondary monazite. The
29 results obtained in the carbonatites of Fuerteventura underscore the interest in studying the concentrations
30 of critical elements, such as REEs, within a non-conventional geological setting like oceanic islands.
31 However, due to intricate structural attributes, the irregular distribution of these mineralizations, and
32 possible land use and environmental constraints, additional future detailed investigations are imperative to
33 ascertain the real potential of these REE concentrations.

34
35
36 **Keywords.** Fuerteventura, Canary Islands, Oceanic Island, Rare earth elements, Carbonatites

37 **1 Introduction**

38 The European Commission (EC) is spearheading efforts to combat climate change through the European
39 Green Deal (EGD), with the goal of achieving a carbon-neutral continent by 2050 (European Commission,
40 2019). This initiative entails transitioning to green technologies, which heavily rely on rare earth elements
41 (REEs) for applications like renewable energy systems and electric vehicles. (Acosta-Mora et al., 2018;
42 Alonso et al., 2012; Chakhmouradian and Wall, 2012; Massari and Ruberti, 2013; Méndez-Ramos et al.,
43 2013; Wondraczek et al., 2015).

44 According to the International Union of Pure and Applied Chemistry (IUPAC), REEs comprise a group of
45 17 chemical elements: scandium (Sc), yttrium (Y) and the 15 members of the lanthanide series (Connelly
46 et al., 2005). The term “rare” is confusing because, even though REEs seldom occur in pure mineral phases,
47 their average concentration in the Earth’s crust is around 125 ppm, surpassing other metals such as copper,
48 gold or platinum (Long et al., 2010; Rudnick and Gao, 2014).

49 Given their pivotal role in modern industry and green technologies, as well as the projected increase in
50 demand for REEs in the coming years, governments worldwide are actively promoting the advancement of
51 knowledge regarding REE distribution in the geological environment (Barteková and Kemp, 2016;
52 European Commission, 2023a; European Commission, 2023b).

53 The study of REEs has primarily centred on investigating non-conventional HREE geological settings such
54 as soils and weathering products (Braun et al., 1993; Wang et al., 2010, Wang et al., 2013; Berger et al.,
55 2014; Aiglsperger et al., 2016; Torró et al., 2017; Reinhardt et al., 2018; Borst et al., 2020), but also
56 traditional and well-known LREE-bearing lithologies, such as carbonatites (Goodenough et al., 2016; Yang
57 et al., 2019; Pirajno and Yu, 2022).

58 Carbonatites are igneous rocks formed by carbonate mantle melts and are genetically associated with a
59 wide range of mafic, ultramafic, and alkaline silicate rocks (Yaxley et al., 2002). Although carbonates such
60 as calcite or dolomite are their main forming minerals, a significant portion of carbonatites contain
61 accessory phases enriched in critical metals such as REEs (Christy et al., 2021). REEs can be contained in
62 fluorcarbonates (e.g., bastnäsite, parisite, huanghoite, synchysite), phosphates (e.g., monazite,
63 rhabdophane), silicates (e.g., allanite), or even oxides (e.g., REE-bearing pyrochlore, cerianite). These
64 accessory minerals make carbonatites the main current REE source, representing 86.5% of the deposits
65 under exploitation for these elements (Liu et al., 2023). However, although carbonatites are rare rocks,
66 predominantly found in continental rifts associated with cratons (Humphreys-Williams et al., 2021), they

67 have exceptionally been described in other geological contexts, most notably oceanic islands associated
68 with hotspots, such as Cape Verde (Mourão et al., 2010; De Ignacio et al., 2018;) or Fuerteventura in the
69 Canary Islands (Mangas et al., 1996; Carnevale et al., 2021).

70 The petrogenesis of carbonatites is still a debated topic (Anenburg et al., 2021; Yaxley et al., 2022).
71 Different processes have been proposed for their formation, although there is a consensus that they originate
72 from primary fusion processes derived from a carbonated mantle (Kamenetsky et al., 2021). For the specific
73 case of the oceanic carbonatites, this debate is even more lively. Doucelance et al. (2010) suggested a
74 shallow origin from low-degree partial melting at the base of the oceanic lithosphere. Other authors have
75 proposed the involvement of unmixing process linking to alkaline magma suites (Weidendorfer et al.,
76 2016), the action of hydrothermal fluids of marine origin enriched in Ca that would have serpentinized the
77 mantle (Park and Rye, 2013) or even the contribution of recycled marine carbonates through subduction or
78 assimilated in shallow magma chambers (Démeny et al., 1998; Hoernle et al., 2002; Doucelance et al.,
79 2014).

80 The present study focuses on the mineralogical and geochemical analysis of carbonatites and associated
81 alkaline igneous rocks, as well as their weathering products, in three distinct sectors in the western region
82 of Fuerteventura (Canary Islands, Spain; see Figure 1). The primary objective of this research is to deepen
83 our understanding of REE distribution in these materials, within the exotic geological context of an oceanic
84 island associated with intraplate magmatism.

85

86 **2 Geological setting**

87 **2.1 The Canary Island Seamount Province**

88 The Canary Islands archipelago, located between 27°N and 30°N of latitude, is part of the Canary Island
89 Seamount Province (CISP). This volcanic region forms a band of approximately 1300 km in length and
90 350 km in width, running parallel to the African continental margin. Within the CISP, there are over 100
91 seamounts and up to 8 emerged islands: El Hierro, La Palma, La Gomera, Tenerife, Gran Canaria,
92 Lanzarote, Fuerteventura and Savage islands (Courtilot et al., 2003; Schmincke and Sumita, 2010; van den
93 Bogaard, 2013). Based on magnetic anomaly measurements and dating of both emerged and submarine
94 igneous materials, volcanic activity in the CISP spans more than 142 Ma, from the Early Cretaceous to the
95 present day (Frisch, 2012; van den Bogaard, 2013; Longpré and Felpeto, 2021).

96 **2.2 Fuerteventura Island**

97 Fuerteventura, the easternmost island of the Canarian archipelago, along with Lanzarote, forms the
98 emergent crest of the Eastern Canarian Volcanic Ridge, which is located approximately 100 km offshore
99 from the Moroccan coast (Figure 1). Fuerteventura is the oldest island in the archipelago, with its initial
100 stages of formation linked with submarine volcanic activity, dating to the Oligocene (~34 Ma). The first
101 episodes of subaerial volcanism occurred around ~23 Ma (Coello, 1992; Ancochea et al., 1996; Pérez-
102 Torrado et al., 2023).

103 Fuerteventura is characterized by the occurrence of three distinct main geological units, arranged in order
104 from oldest to youngest: the Fuerteventura basal complex (FBC), the Miocene subaerial volcanic units, and
105 the Pliocene-Quaternary volcano-sedimentary facies (Fúster et al., 1968; Le Bas et al., 1986; Muñoz et al.,
106 2005; Gutiérrez et al., 2006; Troll and Carracedo, 2016).

107

108 **2.2.1 The Fuerteventura basal complex**

109 The FBC unit mainly outcrops in the western part of the island (Figure 1). Two different groups of
110 lithofacies may be distinguished: (1) Early Jurassic to Late Cretaceous oceanic crust materials (Steiner et
111 al., 1998), constituted by mid-ocean ridge basalts and oceanic sediments; (2) Oligocene submarine and
112 transitional volcanic rocks associated with plutonic bodies and dyke swarms (Feraud et al., 1985; Hobson
113 et al., 1998; Gutiérrez et al., 2006). In this second group, a set of lithologies can be distinguished related to
114 an ultra-alkaline-carbonatitic magmatic pulse that occurred ~25 Ma (Le Bas, 1981; Barrera et al., 1986;
115 Balogh et al., 1999). Additionally, alkaline ultramafic, mafic and felsic plutonic rocks such as wehrlites,
116 pyroxenites, gabbros and syenites intruded the previously existing Oligocene materials, forming distinctive
117 ring complexes (Muñoz et al., 2005). These magmatic rocks, predominantly of Oligocene age, have been
118 interpreted as episodes of submarine and transitional growth in Fuerteventura (Le Bas et al., 1986; Gutiérrez
119 et al., 2006).

120 In general, outcrops related with the FBC intrusive assemblage exhibit significant variations and four
121 distinct morphologies and characteristic textures can be identified (Fúster et al., 1968; Barrera et al., 1986;
122 Le Bas et al., 1986; Fernández et al., 1997; Mangas et al., 1992, 1994, 1997; Ahijado 1999; Ancochea et
123 al., 2004; Ahijado et al., 2005; Muñoz et al., 2005):

- 124 (1) Basaltic, alkaline and carbonatitic dykes and veins of meter-scale, decimeter-scale, and
125 centimeter-scale, that are randomly distributed, resulting in a chaotic arrangement (Figure 2a, b).
126 Related to the carbonatite veins and dikes, an intense fenitization may occur.
- 127 (2) Shear zones (Fernández et al., 1997), characterized by gradual or diffuse boundaries, which
128 display assimilation structures between different rock bodies, along with the presence of
129 mylonites, and brecciated textures resulting from deformation (Figure 2c).
- 130 (3) Pegmatitic textures developed within certain rock bodies, often containing centimeter-sized
131 crystals of rock-forming minerals (Figure 2d).
- 132 (4) Contact metamorphism and metasomatism, as well as skarn zones that occur in deformed or
133 undeformed carbonatites, influenced by subsequent hydrothermal fluid circulation (Ahijado et al.,
134 2005; Casillas et al., 2008, 2011).

135

136 In addition, during Miocene magmatic pulses, alkaline plutons were formed in the central-western part of
137 Fuerteventura Island north of the locality of Pájara (sector 2, Figure 1). These intrusions constitute typical
138 ring complexes of alkaline magmatic rocks, including nepheline syenites, syenites, and trachytes (Muñoz,
139 1969). They are regarded as the most recent rocks in the FBC (Figure 1) and have been dated using the K-
140 Ar method, yielding an approximate age of 20.6 ± 1.7 Ma (Le Bas et al., 1986; Holloway and Bussy, 2008).

141

142 **2.2.2 Miocene subaerial volcanic unit**

143 During the Miocene, Fuerteventura witnessed the formation of up to three volcanic edifices (Figure 1;
144 Coello et al., 1992; Ancochea et al., 1996). The northern volcanic structure, referred to as the Tetir edifice,
145 experienced two volcanic construction phases between 22 and 12.8 Ma (Balcells et al., 1994). These
146 episodes involved the eruption of basalts, picritic basalts, oceanic basalts, trachybasalts and trachytes. In
147 the central part of the island, the Gran Tarajal edifice developed three different construction phases
148 spanning from 22.5 to 14.5 Ma (Balcells et al., 1994). On the Jandía Peninsula, in the southern part of the
149 island, a volcanic edifice comprising both basaltic and trachybasaltic materials emerged. It formed three
150 successive construction episodes occurring between 20.7 and 14.2 Ma ago (Balcells et al., 1994). Based on
151 their mineralogical and petrological features, the lithologies comprising this unit have not been considered
152 as potentially containing significant concentrations of REEs. Therefore, they have not been included in the
153 present study.

154

155 **2.2.3 Pliocene and Quaternary volcano-sedimentary facies**

156 After the subaerial volcanic activity during the Miocene, a period of volcanic quiescence ensued, leading
157 to the erosion of the previously formed volcanic edifices. Subsequently, during the Pliocene (between 5.3
158 and 2.6 Ma), a phase of magmatic rejuvenation began, characterized by scattered Strombolian eruptions
159 (Figure 1). Concurrently, various sedimentary formations emerged across the entire island, including littoral
160 and shallow-water marine deposits, as well as aeolian, colluvial, and alluvial subaerial sediments and
161 paleosols from the Pliocene to the Quaternary (Fúster et al., 1968; Zazo et al., 2002; Ancochea et al., 2004).
162 The soils on Fuerteventura are predominantly classified as eutric cambisols and lithosols-vitric andosols,
163 according to the FAO/UNESCO (1970) nomenclature. However, the current arid and deforested conditions
164 have led to extensive erosion of the weathered rock profiles present in different areas of the island. Edaphic
165 calcretes are abundant in Fuerteventura (Chiquet et al., 1999; Alonso-Zarza and Silva, 2002; Huerta et al.,
166 2015; Alonso-Zarza et al., 2020). These formations consist of laminar horizons comprising centimeter-
167 thick layers of micritic calcite, occasionally interspersed with brecciated structures, alongside detrital
168 siliciclastic grains and palygorskite (Alonso and Silva 2002). Petrological and geochemical analyses
169 suggest that these calcretes originated from aeolian dust deposition, with intermittent periods of leaching
170 and calcite precipitation during wetter conditions, wherein biological activity played a significant role in
171 carbonate precipitation (Huerta et al., 2015). Trace element concentrations also indicate that calcium-
172 bearing minerals from the volcanic host rock have a negligible contribution to calcrete formation, with the
173 majority of calcium being supplied by aeolian deposits, such as dust from the Sahara and Sahel deserts
174 (Goudie and Middleton, 2001; Menéndez et al., 2007; Scheuven et al., 2013; Huerta et al., 2015).

175

176

177 **3 Materials and Methods**

178 **3.1 Sampling**

179 Alkaline magmatic rocks and especially carbonatites are considered potential targets for the exploration of
180 rare earth elements (Goodenough et al., 2016; Balaram et al., 2019; Anenburg et al., 2021; Beland and
181 Jones, 2021). In Fuerteventura, these types of lithologies are found in two distinct geological areas: the
182 Oligocene (sectors 1 and 3; Figure 1) and the Miocene lithologies related with the FBC (sector 2, Figure
183 1).

184 Considering that weathering profiles may concentrate REE in larger quantities than primary bedrocks (Bao
185 and Zhao, 2008; Menéndez et al., 2019, Braga and Biondi, 2023; Chandler et al., 2024), these lithological
186 formations were included in the present study and sampling was conducted on a selection of six different
187 profiles: (1) Agua Salada ravine (sector 1) and (2) Aulagar ravine (sector 3), hosted by carbonatites, (3) the
188 FV-30 road, (4) Las Peñitas quarry, (5) Palomares ravine and (6) the Pájara profiles, on syenite bedrock
189 (Figure 1; Table S1).

190 Accordingly, a systematic sampling campaign was conducted in three different sectors of Fuerteventura,
191 targeting alkaline and carbonatitic igneous rocks and their associated weathering products. The specific
192 locations of these predetermined sectors are outlined in Figure 1. As a result, a set of 29 representative
193 samples of potentially REE-enriched magmatic rocks, along with 21 samples of associated weathering
194 products, were collected for further analysis (Table S1). For the weathering products, we conducted six
195 sampling profiles (labelled A to F; Figure 1) at various suitable points to compare the mineralogical and
196 geochemical changes resulting from weathering of the primary magmatic rocks.

197

198 **3.2 Petrographic and mineralogical studies**

199 Selected samples of magmatic rocks were prepared in thin sections for textural and mineralogical analysis
200 at the Laboratory of Geological and Paleontological Preparation of the Natural Sciences Museum of
201 Barcelona (LPGiP-MCNB; Barcelona, Spain). A representative subset of these samples was also examined
202 using a JEOL JSM-7100 field emission scanning electron microscope (FE-SEM) at the Scientific and
203 Technological Centers of the Universitat de Barcelona (CCiTUB). The FE-SEM system is equipped with
204 an INCA Pentaflex EDS (energy dispersive spectroscopy) detector (Oxford Instruments, England), which
205 allowed for the acquisition of semi-quantitative analyses of mineral phases. The general operating
206 conditions for the FE-SEM were a 15-20 kV accelerating voltage and a 5 nA beam current.

207 To achieve accurate and precise mineralogical identification and characterization of the weathering
208 magmatic rocks and calcretes, X-ray powder diffraction (XRPD) measurements were performed using a
209 PANalytical Empyrean powder diffractometer equipped with a PIXcel1D Medipix 3 detector at the
210 Integrated XRD Service of the General Research Support Service of La Laguna University, Spain. The
211 diffractometer employed incident Cu K_{α} radiation at 45 kV and 40 mA, along with an RTMS (real-time
212 multiple strip) PIXcel1D detector with an amplitude of $3.3473^{\circ} 2\theta$. The diffraction patterns were obtained
213 by scanning random powders in the 2θ range from 5° to 80° . Data sets were generated using a scan time of

214 57 seconds and a step size of 0.0263° (2θ), with a $1/16^\circ$ divergence slit. Mineral identification and semi-
215 quantitative results were obtained using the PANalytical's HighScore Plus search-match software (v. 4.5)
216 with a PDF+ database.

217

218 **3.3 Geochemical analyses**

219 The major elements composition of carbonates from carbonatites was studied using an electron probe
220 microanalyzer (EPMA) system. The EPMA analyses were conducted on a JEOL JXA-8230 electron
221 microprobe, equipped with five wavelength-dispersive spectrometers and a silicon-drift detector EDS,
222 located at the CCiTUB. The spot mode was employed for the analyses and the electron column was set to
223 an accelerating voltage of 15 kV and a beam current of 10 nA. Standard counting times of 10 seconds were
224 used, along with a focused beam, to achieve the highest possible lateral resolution. The analytical standards
225 employed during the analysis process were: celestine (PETJ, Sr K_α), wollastonite (PETL, Ca K_α), periclase
226 (TAPH, Mg K_α), hematite (LiFH, Fe K_α), rhodonite (LiFH, Mn K_α) and albite (TAPH, Na K_α).

227 Bulk-rock geochemical data of major and trace element composition were obtained by X-ray fluorescence
228 (XRF) and inductive coupled plasma (ICP)-emission spectrometry. The samples were prepared by lithium
229 metaborate/tetraborate fusion and nitric acid digestion at the ACTLABS Activation Laboratories Ltd.
230 (Ancaster, Canada).

231

232 **4 Results**

233 **4.1 Petrography and mineralogy**

234 **4.1.1 Alkaline magmatic rocks and carbonatites**

235 The primary lithologies under study, consist of Oligocene (~ 25 Ma) alkaline igneous and carbonatitic rocks,
236 as well as Miocene alkaline lithologies (K–Ar age of 20.6 ± 1.7 Ma; Le Bas et al., 1986), that form part of
237 the FBC. Their outcrops extend across kilometer-scale areas but exhibit high heterogeneity at a detailed
238 level due to the occurrence of numerous small intrusions, ranging in size from metric to decimetric
239 dimensions (Figs. 2a, b).

240 At a mineralogical level, separation of the different types of alkaline rocks found in the FBC is complex
241 because these lithologies are intimately associated and infiltrate diffusely, leading to the formation of hybrid
242 intrusions. The materials with the most mafic composition correspond to pyroxenites and melteigites, and
243 their formation is associated with the earliest magmatic fractions. However, these are commonly spatially

244 associated with more differentiated rocks, mainly ijolites, nepheline syenites, and syenites. All these
245 lithologies have a relatively simple mineralogy, characterized by varying proportions of nepheline (10-30%
246 modal) and potassium feldspar (50-80% modal), associated with aegirine-augite and biotite (10-30%
247 modal). A set of accessory minerals with varying proportions (always less than 5% modal) also occur,
248 including ilmenite, titanite, zircon, and fluorapatite.

249 At a textural level, the alkaline series lithologies of the FBC present granular textures with millimeter-sized
250 euhedral grains. However, in some of the intrusions in sectors 2 and 3, pegmatitic syenites-ijolites were
251 detected with centimeter-sized grains characterized by the presence of large aegirine-augite crystals.

252 Some of the intrusions described in the three sectors show aphanitic textures caused by faster cooling,
253 resulting in rocks with similar mineralogy but extrusive-type textural characteristics. Therefore, due to their
254 textural features, some dikes and apophyses, although mineralogically equivalent, should be classified as
255 trachytes and phonolites.

256 Carbonatitic intrusions commonly co-occur with the alkaline rocks, sharing similar morphology, textures,
257 and spatial distribution within the outcrops (Figure 2e). Furthermore, alkaline and/or carbonatitic intrusions
258 can be occasionally associated with mafic intrusions, primarily pyroxenites and alkaline gabbros. In
259 addition, a subsequent set of mafic dikes with basaltic composition overlaps the previous intrusive bodies
260 (Figs. 2a, b).

261 All carbonatites described in different outcrops from sectors 1 and 3 are predominantly composed of calcite
262 (95% modal) and can thus be classified as calciocarbonatites (Le Maitre, 2005). None of the studied samples
263 shows the occurrence of ferromagnesian carbonates such as ankerite, dolomite, and/or siderite, as well as
264 REE carbonates. Texturally, calcite occurs as euhedral crystals ranging in size from millimetres to
265 centimetres, often recrystallized and exhibiting polysynthetic twinning. In some cases, a secondary micritic
266 calcite matrix is present, filling interstitial spaces and fractures.

267 The major element composition of calcite is relatively consistent across all the carbonatite samples.
268 Notably, there are significant contents of SrO, with values of up to 5.43 wt%, while REEs are absent from
269 the carbonate composition (Table S2).

270 The accessory mineralogy (~5% modal) comprises disseminated phases within the calcium carbonate.
271 Among them, the occurrence of minerals from the spinel group, including magnetite (Figure 3a), and
272 primarily jacobsonite, occurring as subhedral crystals of up to 50 μm (Figure 3b). Another characteristic
273 mineral is perovskite, occurring as subhedral crystals of up to 100 μm . These grains are remarkable for

274 their significant Nb contents, as described in other carbonatitic localities worldwide (Torró et al., 2012).
275 Britholite also occurs as subhedral crystals of up to 100 μm (Figure 3b). This primary britholite contains
276 significant LREE content (Figure 4), and its alteration leads to the formation of secondary REE-enriched
277 phosphates, mainly monazite-Nd (Figure 3c), which also contains substantial amounts of La and Ce (Figure
278 4). REEs, in addition to occurring in primary britholite and secondary monazite, were also detected in tiny
279 pyrochlore grains, heterogeneously disseminated in the calcite groundmass (Figure 3b). In some cases,
280 pyrochlore forms euhedral crystals of up to 20 μm , also included in calcite (Figure 3d). This pyrochlore
281 shows slight zoning towards plumbopyrochlore (Christy and Atencio, 2013), with significant enrichment
282 in Pb observed at grain borders (Figure 3d).

283 Carbonatites can be affected by certain contact metamorphism, especially in sectors 1 and 3 (Figure 1) and
284 may exhibit a slightly different mineralogy from the one described thus far. This is characterized by the
285 occurrence of skarn-type metamorphic minerals, formed due to the interaction between carbonatites and
286 spatially associated silica-rich rocks. Among these minerals, there are subhedral crystals of andradite, up
287 to 30 μm in size, implanted in a matrix of secondary calcite and phlogopite, exhibiting pronounced zoning
288 with kerimasite cores (Figure 3e). In these areas, the occurrence of REE mineralizations associated with
289 allanite (Figure 3f) is also typical. Allanite occurs as granular aggregates associated with hydrothermal
290 secondary sulfates, primarily baryte (Figure 3f), but occasionally celestine (Figure 3c).

291 This particular mineralogy, typically associated with skarn formations, emerges from the interaction
292 between a carbonatite intrusion and surrounding silicate rocks, in contrast to the typical process. It has
293 recently gained attention from several researchers in various carbonatite locations worldwide, who have
294 coined the term antiskarn to describe it (Anenburg and Mavrogenes, 2018; Yaxley et al., 2022).

295

296 **4.1.2 Weathering products**

297 In certain areas within the three studied sectors (Figure 1), there is evidence of the development of
298 characteristic shallow geological formations consistently associated with weathering, which affect the
299 outlined magmatic lithologies (Figs. 5, 6). These geological products were studied through the analysis of
300 six alteration profiles, developed on carbonatites (Agua Salada and Aulagar) and syenites (Palomares
301 ravine, FV-30 road, Las Peñitas quarry, and Pájara) (Figure 1).

302 The calcrete and carbonatite section generally consist of centimetre-scale calcrete veins injected into the
303 carbonatitic host rock (Figure 5). In general, the development of weathering products was not detected on
304 carbonatites in any of the studied sectors of the FBC.

305 Weathering products developed on syenite bedrock are generally more abundant. The cambic B horizon
306 displays reddish to yellowish colorations (5YR6/6), with a thickness of up to 20-30 cm. Additionally, it is
307 common to find BC horizons instead of B horizons, while the C horizon is well-developed, reaching a 30-
308 40 cm thickness at certain levels of the profile (Figure 6). Furthermore, except for the Las Peñitas profile
309 (E profile, Figure 1), centimetre-scale calcrete bands (Bk; Jahn et al., 2006) were also detected in deeper
310 layers across all the studied profiles.

311 In terms of mineralogical composition, carbonatite profiles exhibit significant changes due to weathering.
312 In general, weathering processes lead to a reduction in calcite, the disappearance of fluorapatite, and the
313 formation of secondary minerals like palygorskite (Figure 7). The contribution from lateral slope movement
314 is also evident through the presence of residual plagioclase and clinopyroxene.

315 In the case of syenite weathering profiles, illite/chlorite and kaolinite are the predominant secondary
316 products, followed by muscovite and palygorskite (Figure 7). Other minerals such as quartz were also
317 detected, even in the C horizons.

318

319 **4.2 Bulk-rock and mineral geochemistry**

320 Chemical analysis of the major, minor and trace elements were carried out in order to evaluate the
321 geochemical features and the distribution of REEs, on 25 representative samples of igneous rocks from the
322 FBC, including trachytes, phonolites, syenites, ijolites and carbonatites (Table S3). In addition, we also
323 analysed 21 samples of weathering products (Table S4).

324 The total REY (REEs plus yttrium) content in the FBC igneous rocks exhibits widespread and significant
325 enrichment in comparison to the average crustal values (~125 ppm, Rudnick and Gao, 2014). Notably, the
326 extrusive and magmatic alkaline lithologies (trachytes and phonolites as well as syenites and ijolites) show
327 variable REY values ranging between about 230 and 1,400 ppm (Table S3). In contrast, the carbonatitic
328 rocks exhibit REY content more than ten times greater than the alkaline lithologies, with specific samples
329 reaching maximum values of up to about 10,300 ppm, as evidenced in sample 85a sourced from a
330 carbonatite outcrop in sector 1 (Table S3).

331 The weathered magmatic rocks, though moderately significant in REY content relative to the average
332 crustal values (Table S4), still exhibit slightly lower levels compared to the content observed in the
333 associated alkaline and carbonatitic protoliths (Table S3). A contrasting pattern emerges in the calcretes,
334 where REY values experience a sharp reduction, presenting virtually negligible values ranging between 20
335 and 72 ppm REY. These levels are significantly below the average Earth's crust values (Rudnick and Gao,
336 2014) and are markedly lower than those observed in both the alkaline lithologies and, particularly, the
337 carbonatites of the FBC.

338 REE normalized diagrams further underscore this distribution, portraying elevated content in the
339 carbonatites, followed by the alkaline rocks (Figure 8a). Meanwhile, the weathered magmatic rocks and
340 calcretes (Figure 8b) display significantly lower values. All studied lithologies exhibit clear negative
341 patterns, indicative of enrichment in LREEs relative to HREEs. Notably, carbonatites and alkaline rocks
342 (Figure 8a) exhibit a flattening of these negative patterns in the final segment, indicating a certain degree
343 of HREE enrichment.

344 The FCB carbonatites exhibit a depletion in some critical elements commonly associated with this lithology
345 such as Nb or Ta (Table S3). Negative anomalies of both Nb and Ta are clearly observed in the multi-
346 element diagrams of carbonatite samples (Figure 9a). However, given the presence of pyrochlore in the
347 carbonatites, these anomalies in Nb and Ta are likely not indicative. We interpret that the low concentrations
348 of these elements could be attributed to an analytical artifact that would underestimate the contents of High
349 Field Strength Elements (HFSE) due to the challenge of pyrochlore dissolution in the analytical digestion
350 protocols employed. These protocols have been primarily devised to assess the contents of REEs rather
351 than HFSE. Additionally, alkaline rock patterns also show a distinctive negative anomaly in Sr (Figure 9b).
352 As for the weathering products, their contents of other minor elements do not indicate significant
353 concentrations of metals or critical elements like Nb or Ta (Table S4). The multi-element diagrams for the
354 calcretes exhibit a negative Ta anomaly (Figure 9c), while the patterns of weathered magmatic rocks do not
355 reveal notable anomalies in any group of elements (Figure 9d).

356 A specific geochemical study of REE distribution in the six studied weathering profiles was also conducted
357 (Figure 10). The main objective was to evaluate the geochemical interactions between the protolith and the
358 related weathering lithologies, with the aim of detecting potential REE enrichments or depletions caused
359 by weathering processes.

360 In the exchange patterns of calcretes occurred within carbonatitic host rocks, as analyzed in the Agua Salada
361 and Aulagar ravine profiles (Figs. 10A, B), REE concentrations are two orders of magnitude lower than in
362 the carbonatite (Figure 10A), as also previously determined from the REE diagrams (Figure 8). Notably, it
363 was observed that the concentration of Rare Earth Elements (REE) is directly correlated with the distance
364 from the host rock. This is evident in calcrete sample 14 (Figure 10B), which is situated closer to the
365 carbonatites and exhibits a slight enrichment in REE concentrations (~51.3 ppm Σ REY; Table S4)
366 compared to samples 15 and 18 (Figure 10B), which are located farther away from the carbonatite host
367 rock and show a slight depletion in REE (~20.1 to ~32.6 ppm Σ REY; Table S4). In addition, although the
368 values of all elements are depleted in the calcrete patterns, there is a greater depression in LREE than in
369 HREE relative to the protolith, resulting in typically positive patterns, except for sample 76 from the Agua
370 Salada ravine, where a clear inverse trend is observed (Figure 10A).

371 In general, the diagrams in Figure 10 show that weathering products on syenites exhibit enrichment relative
372 to the protolith (green areas in Figs. 10C, D, E). However, calcrete samples, whether developed on
373 carbonatites or syenites, consistently show depletions compared to the protolith contents (reddish areas in
374 Figs. 10C, D, F). The diagrams corresponding to the weathering products generated on syenites exhibit
375 similar morphologies (Figs. 10C, D, E, F). Overall, these lithologies are characterized by enrichment in
376 REEs relative to the protolith as well as V-shaped patterns, featured by the presence of a negative anomaly
377 in Eu, which is also reported in all C and B horizons developed on syenites, except sample 61 (Figure 10C),
378 and is likely related to plagioclase crystallization.

379

380 **5 Discussion**

381 **5.1 REE distribution on the FBC magmatic rocks**

382 The FBC magmatic rocks, in the three study sectors, encompass alkaline lithologies (trachytes, phonolites,
383 syenites, melteigites, and ijolites) as well as carbonatites. Regarding the group of alkaline rocks, the
384 detected REE content varies between 214 and 1,330 ppm (Table S3), significantly higher than the average
385 concentration determined in the Earth's crust (~125 ppm, Rudnick and Gao, 2014). However, this finding
386 is not surprising, and the observed values in Fuerteventura are not anomalous, as these types of lithologies
387 typically exhibit REE concentrations within this range (Dostal, 2017). Therefore, the measured REE
388 concentrations are neither significant nor sufficiently elevated to hypothetically consider these lithologies
389 as a potential non-conventional deposit of these critical elements in the FBC.

390 On the other hand, FBC carbonatites present significantly higher values in terms of REE content. In the
391 studied carbonatite samples from sectors 1 and 3 (carbonatites do not outcrop in sector 2), REE content
392 ranges between about 1300 ppm and 10,300 ppm. The latter value corresponds to the richest REE-detected
393 sample in the entire FBC, which is located in the Agua Salada ravine area of sector 1 (Table S3; Figure 1).
394 The reported REE content values in the FBC carbonatites are similar to the general average concentrations
395 found in other locations worldwide where carbonatites are exploited for REE extraction. This is the case,
396 for example, of Bayan Obo, the largest REE deposit in the world (Lai et al., 2015; Liu et al., 2018). In this
397 locality, high-grade carbonatites exhibit average concentrations of 2880 ppm (Wu et al., 2008; Smith et al.,
398 2015, 2016), which are equivalent to those measured in some of the samples from Fuerteventura. It should
399 be noted that low-grade carbonatite ore from Bayan Obo presents extremely high values in comparison to
400 the FBC, with REE concentrations reaching 30,750 ppm (Chao et al., 1997; Smith et al., 2016).

401 Another significant example is the Mountain Pass carbonatite in California, USA (Olson et al., 1954; Haxel,
402 2005). In this REE deposit, average value across the whole complex are around 2580 ppm (Castor et al.,
403 2008; Mariano and Mariano, 2012; Smith et al., 2016), also in line with REE concentrations detected in the
404 present study for the FBC carbonatites.

405 This comparative analysis can also be carried out using normalized REE values (Figure 11). In this regard,
406 FBC carbonatites are significantly depleted in LREE compared to those from Bayan Obo (Yang et al.,
407 2019) and Mountain Pass (Castor et al., 2008), although they show similar values to other REE deposits
408 associated with carbonatites, such as those in Ashram, Canada (Beland and Jones, 2021) and Bear Lodge,
409 USA (Moore et al., 2015; Smith et al., 2016; Figure 11). However, the pattern of the Fuerteventura
410 carbonatites exhibits a slightly less pronounced slope, indicating a higher relative content of HREE, which
411 are considered the materials with the highest risk of supply among all the CRMs defined by the EC
412 (European Commission, 2023a). In fact, in the FBC carbonatites, the normalized HREE values are
413 equivalent to those reported in the primary carbonatitic rocks from the deposits of Bayan Obo (China) and
414 Mountain Pass (USA) (Figure 11). The relative significant HREE content reported in FBC carbonatites
415 holds particular significance. The use of HREEs, such as Yb, Er, and Tm, is of particular interest in cutting-
416 edge photonic and nanotechnology applications.

417 At the mineralogical level, it was observed that, in the FBC carbonatites, the main REE-hosting minerals
418 are accessory phases; primarily minerals from the pyrochlore group, found as disseminated euhedral micro-
419 crystals implanted in primary calcite (Figs. 3b, d). Another REE-bearing mineral in the FBC carbonatites

420 is britholite, which exhibits significant LREE content. However, this mineral is commonly altered to
421 monazite (Figs. 3c, 4), interpreted as a secondary phase but also a carrier of these critical elements (Chen
422 et al., 2017).

423 Another noteworthy aspect is the lack of REE fluorcarbonates like bastnäsite $\text{REE}(\text{CO}_3)\text{F}$, parisite
424 $\text{Ca}(\text{REE})_2(\text{CO}_3)_3\text{F}_2$, synchysite $\text{Ca}(\text{REE})(\text{CO}_3)_2\text{F}$ or huanghoite $\text{Ba}(\text{REE})(\text{CO}_3)_2\text{F}$. They do not occur in the
425 FBC, as they do in other REE deposits associated with, for example, the Bayan Obo carbonatite or the
426 Sulphide Queen carbonatite from Mountain Pass (Castor et al., 2008; Smith et al., 2015, 2016).

427

428 **5.2 REE distribution on the associated weathering products**

429 The weathering materials developed on magmatic rocks, also analysed for their REE concentrations,
430 constitute the remnants of soils that were interpreted as developed under wetter conditions during a humid
431 phase of the oxygen isotope stage 2, spanning from 29 to 20 thousand years BP (Huerta et al., 2016). This
432 period aligns with the last glacial maximum, marked by heightened humidity in the Canary Islands,
433 resulting in slope erosion and the formation of talus flatiron (Gutiérrez-Elorza et al., 2013). Over time, these
434 materials have undergone substantial volume reduction due to human-driven deforestation and erosion,
435 primarily before the 15th century (Machado-Yanes, 1996). Notably, topography plays an essential role in
436 the distribution of these weathering profiles and influences specific physical attributes such as slope
437 (FAO/UNESCO, 1974).

438 The studied weathering products developed on syenite rocks (profiles C, D, E, F; Figs. 1, 7) are classified
439 by FAO/UNESCO (1974) as eutric cambisols, reflecting a Mediterranean climate condition. Indeed, on the
440 African continent, which is adjacent to the Canary Islands, eutric cambisols are primarily found within the
441 tropical subhumid zone, gradually transitioning into the semi-arid zone (FAO/UNESCO, 1974). These
442 syenite weathering profiles exhibit better-preserved characteristics and a more significant extent compared
443 to those studied in carbonatites (profiles A and B; Figs. 1, 7). In general, intensive weathering plays a
444 crucial role in the formation of REE deposits, as these elements tend to be concentrated in such geological
445 formations compared to others leached during the weathering process. This phenomenon is exemplified in
446 several locations worldwide, where REE deposits associated with weathering products occur: for instance,
447 Bear Lodge in the USA (Andersen et al., 2017), Chuktukon and Tomtor in Russia (Kravchenko and
448 Pokrovsky, 1995; Kravchenko et al., 2003; Chebotarev et al., 2017), Las Mercedes in the Dominican
449 Republic (Torró et al., 2017), Araxá in Brazil (Braga and Biondi, 2023), and Mount Weld in Australia

450 (Zhukova et al., 2021; Chandler et al., 2024), among many others. However, the weathering processes on
451 Fuerteventura are characterized by fluctuating climatic conditions and intense erosion in the context of a
452 typical Mediterranean climate, which is in turn characterized by drier conditions and a lower propensity for
453 intense weathering compared to tropical climates. The weathering processes on Fuerteventura do not
454 therefore typically lead to the development of laterites and mature weathering profiles, since these
455 conditions do not favor the formation and subsequent preservation of these products, ~~particularly within~~
456 ~~the carbonatite bedrock areas.~~

457

458 **5.3 Fuerteventura carbonatites as potential REE source**

459 Based on the mineralogical and geochemical data, it can be concluded that, among the lithologies studied
460 in the FBC, only the carbonatites are favorable targets for REEs exploration. Therefore, the primary alkaline
461 rocks, as well as the entire suite of corresponding secondary weathering products, can be ruled out.

462 The geochemical data obtained from the oceanic carbonatites of Fuerteventura, exemplified in multielement
463 and REE diagrams (Figure 8), suggest a petrogenetic affinity with carbonatites associated with
464 intracontinental rift geological settings. This similarity has also been previously highlighted by other
465 authors such as Carnevale et al. (2021) who, based on stable isotope data ($\delta^{13}\text{C}$ and $\delta^{18}\text{O}$) and noble gases
466 isotopic composition (He, Ne, Ar), suggested that oceanic and continental carbonatites were comparable in
467 petrogenetic terms. Therefore, despite the lingering questions about the formation processes of oceanic
468 carbonatites, their assessment as a possible source of critical metals, especially REEs, could be considered
469 in the same way as their continental counterparts.

470 However, when considering a more detailed assessment of the sectors where the FBC carbonatites outcrop,
471 it is essential to note that the distribution of these outcrops and thus potential REE mineralization is not
472 straightforward. The carbonatite outcrops have a very limited surface distribution, in the order of metres
473 (Figure 2e), and exhibit complex structural features influenced by shear metamorphism (Figure 2c) and
474 overlapping episodes of intrusive activity that resulted in swarms of dikes with intricate distributions (Figs.
475 2a, b). Hence, these general features of the carbonatite outcrops make it imperative to validly estimate their
476 volume and to carry out more precise studies of their depth distribution.

477 Then, it is important to highlight that any attempt to assess potential REE deposits linked to FBC
478 carbonatites must consider the irregular distribution of these mineralizations. In addition, it should also be
479 considered the existence of regulatory constraints that may stem from the allocation of land for strategic

480 military activities, as well as environmental considerations to safeguard natural and marine-coastal areas,
481 especially bearing in mind that Fuerteventura is a UNESCO biosphere reserve territory. This latter point is
482 particularly pertinent for a specific area within sector 3 (Figure 1). Therefore, any comprehensive analysis
483 of the potential of FBC carbonatites as REE sources must also factor in these potential restrictions tied to
484 land use regulations aimed at upholding the broader socio-economic, environmental, and societal interests
485 inherent to a distinctive site like the island of Fuerteventura.

486

487 **6 Conclusions**

488 A preliminary study of the distribution of REEs was conducted through mineralogical and geochemical
489 analyses of alkaline and carbonatitic igneous rocks within the FBC, along with associated weathering
490 products. Based on the gathered data and their corresponding interpretations, our findings can be
491 summarized as follows:

492 (i) The concentrations of REEs present in the alkaline and carbonatitic rocks of the FBC are
493 significant and exceed the average values attributed to the Earth's crust.

494 (ii) The weathering products developed on these magmatic rocks do not exhibit significant REE
495 enrichment.

496 (iii) Calcified horizons (Bk, calcretes), have practically negligible concentrations of REE
497 elements, being consistent with their sedimentary and aeolian origin reported in the previous
498 literature. Colluvial processes may have influenced the lateral transport and accumulation of
499 REEs in Pleistocene-Holocene deposits distant from the source area.

500 (iv) The detected concentrations of REY in carbonatites range up to about 10,300 ppm, which is
501 a comparable concentration to other locations hosting significant deposits of these critical
502 elements worldwide.

503 (v) Within carbonatites, REEs are primarily hosted in two accessory mineral phases: (1) oxides
504 belonging to the pyrochlore group; and (2) phosphates. In this second group, primary phases
505 such as REE-bearing britholite can be distinguished, as well as monazite generated as a
506 secondary product from the britholite alteration.

507 (vi) Primary calcite in the Fuerteventura carbonatites is not the predominant host of REEs. It
508 displays a highly homogeneous composition with insignificant Fe-Mg content and negligible
509 REEs.

510 (vii) The complex structural features of the studied FBC outcrops (deformation, metamorphism,
511 swarms of dikes from different intrusive pulses...) make it essential to conduct more detailed
512 studies to quantify real REE resources.

513 (viii) All the studied sectors contain outcrops located in restricted areas due to environmental or
514 military use concerns. Any further detailed analysis of REE distribution in the FBC
515 carbonatites must take into account the environmental, socio-economic, and geostrategic
516 factors.

517

518 **Acknowledgements**

519 This research was funded by the “Tierras Raras” project (SD-22/25) and the “MAGEC-REEmounts”
520 project (ProID-20211010027) of the Canarian Agency for Research, Innovation and Information Society
521 (ACIISI by its initials in Spanish) of the Canary Islands Government. Funding support was also provided
522 by the project “Materials for Advanced Energy Generation” (ENE2013-47826-C4-4-R), “3D Printed
523 Advanced Materials for Energy Applications” (ENE2016-74889-C4-2-R) and “Estudio de los procesos
524 magmáticos, tectónicos y sedimentarios involucrados en el crecimiento temprano de edificios volcánicos
525 oceánicos en ambiente de intraplaca” (CGL2016-75062-P), all funded by the Government of Spain. The
526 collection of samples in specific protected areas required authorization from the Fuerteventura Island
527 Government. We appreciate the cooperation and assistance provided by the Spanish Army, especially by
528 the soldier Liberto Yeray Puga Acosta, who facilitated our access to the Pájara CMT restricted military
529 area to carry out sampling. We thank Gerard Lucena from the LPGiP-MCNB for his thorough work in the
530 elaboration of polished thin sections. We would also like to express our acknowledgements to professor
531 Michael Anenburg, an anonymous reviewer, and editors Johan Lissenberg and Andrea Di Muro for their
532 constructive and enriching comments and corrections, which greatly improved the initial version of this
533 manuscript

534

535 **Statements and Declarations**

536 **Data availability statement**

537 The authors confirm that the data supporting the findings of this study are available within the article and
538 its supplementary materials.

539

540 **Competing interests**

541 The authors declare no competing interests. The funders had no role in the design of the study, in the
542 collection of samples, the analyses, the interpretation of data, the writing of the manuscript nor the decision
543 to publish these results.

544 **Author contributions**

545 Conceptualization: MC, IM, LQ, JY, JM; fieldwork and sampling: MC, IM, LQ, JY, RC, AA, JM;
546 methodology: MC, IM, JY, JM; validation of results: MC, IM, LQ, JY, RC, JMR, JM; data curation: MC,
547 IM, JM; writing-original draft preparation: MC, IM, JY, JM; writing-review editing: MC, IM, LQ, JY, RC,
548 JMR, JM; supervision: IM, JY, JM; project administration: JMR, JM; funding acquisition: IM, JY, RC,
549 JMR, JM.

550

551 **Additional information**

552 Supplementary tables are available in the online version at <https://XXXXX>

553 **References**

- 554 Acosta-Mora, P., Domen, K., Hisatomi, T., Lyu, H., Méndez-Ramos, J., Ruiz-Morales, J. C., Khaidukov,
555 N. M.: “A bridge over troubled gaps”: up-conversion driven photocatalysis for hydrogen generation
556 and pollutant degradation by near-infrared excitation, *Chem. Commun*, 54, 1905–1908
557 <https://doi.org/10.1039/C7CC09774C>, 2018.
- 558 Aiglsperger, T., Proenza, J. A., Lewis, J. F., Labrador, M., Svojtka, M., Rojas-Purón, A., Longo, F.,
559 Āurišová, J.: Critical metals (REE, Sc, PGE) in Ni laterites from Cuba and the Dominican Republic,
560 *Ore Geol. Rev.*, 73, 127–147, <https://doi.org/10.1016/j.oregeorev.2015.10.010>, 2016.
- 561 Ahijado, A.: Las intrusiones plutónicas e hipoabisales del sector meridional del Complejo Basal de
562 Fuerteventura, Doctoral Thesis, Universidad Complutense de Madrid, 392 p., 1999.
- 563 Ahijado, A., Casillas, R., Nagy, G., Fernández, C.: Sr-rich minerals in a carbonatite skarn, Fuerteventura,
564 Canary Islands (Spain), *Mineralogy and Petrology*, 84, 107–127, <https://doi.org/10.1007/s00710-005-0074-8>, 2005.
- 566 Alonso, E., Sherman, A. M., Wallington, T. J., Everson, M. P., Field, F. R., Roth, R., Kirchain, R. E.:
567 Evaluating Rare Earth Element Availability: A Case with Revolutionary Demand from Clean
568 Technologies, *Environ. Sci. Technol.*, 46, 3406–3414, <https://doi.org/10.1021/es203518d>, 2012.
- 569 Alonso-Zarza, A. M., Silva, P. G.: Quaternary laminar calcretes with bee nests evidences of small-scale
570 climatic fluctuations, Eastern Canary Islands, Spain, *Palaeogeogr. Palaeoclimatol. Palaeoecol.*, 178,
571 119–135, [https://doi.org/10.1016/S0031-0182\(01\)00405-9](https://doi.org/10.1016/S0031-0182(01)00405-9), 2002.
- 572 Alonso-Zarza, A. M., Rodríguez-Berriguete, Á., Casado, A. I., Martín-Pérez, A., Martín-García, R.,
573 Menéndez, I., Mangas, J.: Unravelling calcrete environmental controls in volcanic islands, Gran
574 Canaria Island, Spain, *Palaeogeogr. Palaeoclimatol. Palaeoecol.*, 554, 109797,
575 <https://doi.org/10.1016/j.palaeo.2020.109797>, 2020.
- 576 Ancochea, E., Brändle, J. L., Cubas, C. R., Hernán, F., Huertas, M. J.: Volcanic complexes in the eastern
577 ridge of the Canary Islands: the Miocene activity of the Island of Fuerteventura, *Journal of*
578 *Volcanology and Geothermal Research*, 70, 183–204, [https://doi.org/10.1016/0377-0273\(95\)00051-](https://doi.org/10.1016/0377-0273(95)00051-8)
579 [8](https://doi.org/10.1016/0377-0273(95)00051-8), 1996.
- 580 Ancochea, E., Barrera, J. L., Bellido, F.: Canarias y el vulcanismo neógeno peninsular. *Geología de España*,
581 635-682. In: Aparicio, A., Hernán, F., Cubas, C. R., Araña, V., 2003, Fuentes mantélicas y evolución
582 del vulcanismo canario, *Estudios Geológicos*, 59, 5–13, <https://doi.org/10.3989/egeol.03591-477>,
583 2004.
- 584 Andersen, A. K., Clark, J. G., Larson, P. B., Donovan, J. J.: REE fractionation, mineral speciation, and
585 supergene enrichment of the Bear Lodge carbonatites, Wyoming, USA, *Ore Geology Reviews*, 89,
586 780–807, <https://doi.org/10.1016/j.oregeorev.2017.06.025>, 2017.
- 587 Anenburg, M., Mavrogenes, J.A., Carbonatitic versus hydrothermal origin for fluorapatite REE-Th
588 deposits: experimental study of REE transport and crustal “antiskarn” metasomatism, *American*
589 *Journal of Science*, 318, 335–366, <https://doi.org/10.2475/03.2018.03>, 2018.
- 590 Anenburg, M., Broom-Fendley, S., Chen, W.: Formation of Rare Earth Deposits in Carbonatites, *Elements*,
591 17, 327–332, <https://doi.org/10.2138/gselements.17.5.327>, 2021.

592 Balcells, R., Barrera, J. L., Gómez, J. A., Cueto, L. A., Ancochea, E., Huertas, M. J., Ibarrola, E., Snelling,
593 N.: Edades radiométricas en la Serie Miocena de Fuerteventura (Islas Canarias), *Bol. Geol. Min.*, 35,
594 450–470, 1994.

595 Balaram, V.: Rare earth elements: A review of applications, occurrence, exploration, analysis, recycling,
596 and environmental impact, *Geoscience Frontiers*, 10, 1285–1303,
597 <https://doi.org/10.1016/j.gsf.2018.12.005>, 2019.

598 Balogh, K., Ahijado, A., Casillas, R., Fernández, C.: Contributions to the chronology of the Basal Complex
599 of Fuerteventura, Canary Islands, *Journal of Volcanology and Geothermal Research*, 90, 81–101,
600 [https://doi.org/10.1016/S0377-0273\(99\)00008-6](https://doi.org/10.1016/S0377-0273(99)00008-6), 1999.

601 Bao, Z., Zhao, Z.: Geochemistry of mineralization with exchangeable REY in the weathering crusts of
602 granitic rocks in South China, *Ore Geol. Rev.*, 33, 519–535,
603 <https://doi.org/10.1016/j.oregeorev.2007.03.005>, 2008.

604 Barrera, J. L., Fernández-Santín, S., Fúster, J. M., Ibarrola, E.: Ijolitas-Sienitas-Carbonatitas de los Macizos
605 del Norte de Fuerteventura, *Bol. Geol. Min.*, TXCII-IV, 309–321. ISSN 0366-0176, 1993.

606 Barteková, E., Kemp, R., National strategies for securing a stable supply of rare earths in different world
607 regions, *Resources Policy*, 49, 153–164, <https://doi.org/10.1016/j.resourpol.2016.05.003>, 2016.

608 Beland, C. M. J., William-Jones, A. E.: The mineralogical distribution of the REE in carbonatites: A
609 quantitative evaluation, *Chemical Geology*, 585, 120558,
610 <https://doi.org/10.1016/j.chemgeo.2021.120558>, 2021.

611 Berger, A., Janots, E., Gnos, E., Frei, R., Bernier, F., Rare earth element mineralogy and geochemistry in
612 a laterite profile from Madagascar. *Applied Geochemistry* 41, 218–228,
613 <https://doi.org/10.1016/j.apgeochem.2013.12.013>, 2014.

614 Borst, A. M., Smith, M. P., Finch, A. A., Estrade, G., Villanova-de-Benavent, C., Nason, P., Marquis, E.,
615 Horsburgh, N. J., Goodenough, K. M., Xu, C., Kynický, J., Geraki, K.: Adsorption of rare earth
616 elements in regolith-hosted clay deposits, *Nat. Commun.*, 11, 4386, [https://doi.org/10.1038/s41467-](https://doi.org/10.1038/s41467-020-17801-5)
617 [020-17801-5](https://doi.org/10.1038/s41467-020-17801-5), 2020.

618 Braga, J. M., Biondi, J. C.: Geology, geochemistry, and mineralogy of saprolite and regolith ores with Nb,
619 P, Ba, REEs (+ Fe) in mineral deposits from the Araxá alkali-carbonatitic complex, Minas Gerais
620 state, Brazil, *Journal of South American Earth Sciences*, 125, 104311,
621 <https://doi.org/10.1016/j.jsames.2023.104311>, 2023.

622 Braun, J. J., Pagel, M., Herbillin, A., Rosin, C.: Mobilization and redistribution of REEs and thorium in a
623 syenitic lateritic profile: A mass balance study, *Geochem. Cosmochim. Acta*, 57, 4419–4434.
624 [https://doi.org/10.1016/0016-7037\(93\)90492-F](https://doi.org/10.1016/0016-7037(93)90492-F), 1993.

625 Carnevale, G., Caracausi, A., Correale, A., Italiano, L., Rotolo, S.G., An Overview of the Geochemical
626 Characteristics of Oceanic Carbonatites: New Insights from Fuerteventura Carbonatites (Canary
627 Islands), *Minerals*, 11, 203. <https://doi.org/10.3390/min11020203>, 2021.

628 Casillas, R., Nagy, G., Demény, A., Ahijado, A., Fernández, C.: Cuspidine–niocalite–baghdadite solid
629 solutions in the metacarbonatites of the Basal Complex of Fuerteventura (Canary Islands). *Lithos*
630 105:25–41. <https://doi.org/10.1016/j.lithos.2008.02.003>, 2008.

631 Casillas, R., Démeny, A., Nagy, G., Ahijado, A., Fernández, C.: Metacarbonatites in the Basal Complex of
632 Fuerteventura (Canary Islands). The role of fluid/rock interactions during contact metamorphism and
633 anatexis, *Lithos*, 125, 503–520, <https://doi.org/10.1016/j.lithos.2011.03.007>, 2011.

634 Castor, S. B.: The Mountain Pass rare-earth carbonatite and associated ultrapotassic rocks, California, *The*
635 *Canadian Mineralogist*, 46, 779–806, <https://doi.org/10.3749/canmin.46.4.779>, 2008.

636 Chakhmouradian, A. R., Wall, F.: Rare Earth Elements: Minerals, Mines, Magnets (and More), *Elements*,
637 8, 333–340, <https://doi.org/10.2113/gselements.8.5.333>, 2012.

638 Chao, E. C. T., Back, J. M., Minkin, J. A., Tatsumoto, M., Wang, J., Conrad, J. E., McKee, E. H., Hou, Z.
639 L., Meng, Q. R., Huang, S. G.: The sedimentary carbonate-hosted giant Bayan Obo REE-Fe-Nb ore
640 deposit of Inner Mongolia, China: a corner stone example for giant polymetallic ore deposits of
641 hydrothermal origin, *USGS Bulletin*, 2143, 65, <https://doi.org/10.3133/b2143>, 1997.

642 Chandler, R., Bhat, G., Mavrogenes, J., Knell, B., David, R., Leggo, T.: The primary geology of the
643 Paleoproterozoic Mt Weld carbonatite complex, Western Australia, *Journal of Petrology*, 65, 2,
644 <https://doi.org/10.1093/petrology/egae007>, 2024.

645 Chebotarev, D. A., Doroshkevich, A., Klemd, R., Karmanov, N.: Evolution of Nb- mineralization in the
646 Chuktukon carbonatite massif, Chadobets upland (Krasnoyarsk Territory, Russia), *Periodico di*
647 *Mineralogia*, 86, 99–118, <https://doi.org/10.2451/2017PM733>, 2017.

648 Chen, W., Honghui, H., Bai, T., Jiang, S.: Geochemistry of Monazite within Carbonatite Related REE
649 Deposits, *Resources*, 6, 51, <https://doi.org/10.3390/resources6040051>, 2017.

650 Chiquet, A., Michard, A., Nahon, D., Hamelin, B.: Atmospheric input vs in situ weathering in the genesis
651 of calcretes: an Sr isotope study at Gálvez (Central Spain), *Geochim. Cosmochim. Acta*, 63, 311–323,
652 [https://doi.org/10.1016/S0016-7037\(98\)00271-3](https://doi.org/10.1016/S0016-7037(98)00271-3), 1999.

653 Christy, A. G., Atencio, D.: Clarification of status of species in the pyrochlore supergroup, *Mineralogical*
654 *Magazine*, 77, 13–20, <https://doi.org/10.1180/minmag.2013.077.1.02>, 2013.

655 Christy, A.G., Pekov, I.V., Krivovichev, S.G., The Distinctive Mineralogy of Carbonatites, *Elements*, 17,
656 333–338, <https://doi.org/10.2138/gselements.17.5.333>, 2021.

657 Coello, J., Cantagrel, J. M., Hernán, F., Fúster, J. M., Ibarrola, E., Ancochea, E., Casquet, C., Jamond, C.,
658 Díaz-de-Terán, J. R., Cendrero, A.: Evolution of the Eastern volcanic ridge of Canary Islands based
659 on new K-Ar data, *Journal of Volcanology and Geothermal Research*, 53, 251–274,
660 [https://doi.org/10.1016/0377-0273\(92\)90085-R](https://doi.org/10.1016/0377-0273(92)90085-R), 1992.

661 Connelly, N. G., Hartshorn, R. M., Damhus, T., Hutton, A. T.: Nomenclature of Inorganic Chemistry
662 IUPAC Recommendations 2005, RSC Publishing, Cambridge, ISBN-0-85404-438-8, 2005.

663 Courtillot, V., Davaille, A., Besse, J., Stock, J.: Three distinct types of hotspots in the Earth's mantle, *Earth*
664 *Planet. Sci. Letters*, 205, 295–308, [https://doi.org/10.1016/S0012-821X\(02\)01048-8](https://doi.org/10.1016/S0012-821X(02)01048-8), 2003.

665 De Ignacio, C., Muñoz, M., Sagredo, J., Carbonatites and associated nephelinites from São Vicente, Cape
666 Verde Islands, *Min., Mag.*, 76, 311–355, doi:10.1180/minmag.2012.076.2.05, 2012.

667 Demény, A., Ahijado, A., Casillas, R., Vennemann, T.W., Crustal contamination and fluid/rock interaction
668 in the carbonatites of Fuerteventura (Canary Islands, Spain): A C, O, H isotope study, *Lithos*, 44, 101–
669 115, [https://doi.org/10.1016/S0024-4937\(98\)00050-4](https://doi.org/10.1016/S0024-4937(98)00050-4), 1998.

670 Dostal, J.: Rare Earth Element Deposits of Alkaline Igneous Rocks, *Resources*, 6, 34–46,
671 <https://doi.org/10.3390/resources6030034>, 2017.

672 Doucelance, R., Hammouda, T., Moreira, M., Martins, J.C., Geochemical constraints on depth of origin of
673 oceanic carbonatites: The Cape Verde case, *Geochim. Cosmochim. Acta*, 74, 7261–7282,
674 <https://doi.org/10.1016/j.gca.2010.09.024>, 2010.

675 Doucelance, R., Bellot, N., Boyet, M., Hammouda, T., Bosq, C., What coupled cerium and neodymium
676 isotopes tell us about the deep source of oceanic carbonatites, *Earth Planet. Sci. Lett.*, 407, 175–186,
677 <https://doi.org/10.1016/j.epsl.2014.09.042>, 2014.

678 European Commission: European Green Deal, https://commission.europa.eu/strategy-and-policy/priorities-2019-2024/european-green-deal_en, 2019.

680 European Commission: Study on the Critical Raw Materials for the EU 2023 – Final Report,
681 <https://op.europa.eu/en/publication-detail/-/publication/57318397-fdd4-11ed-a05c-01aa75ed71a1> -
682 <https://doi.org/10.32873/725585>, 2023a.

683 European Commission, Regulation of the European Parliament and of the Council establishing a framework
684 for ensuring a secure and sustainable supply of critical raw materials and amending Regulations (EU)
685 168/2013, (EU) 2018/858, 2018/1724 and (EU) 2019/1020, <https://eur-lex.europa.eu/legal-content/EN/TXT/?uri=CELEX%3A52023PC0160>, 2023b.

687 FAO/UNESCO: Soil Map of the World Project 1:5000000, Chart VII, <https://www.fao.org/soils-portal/data-hub/soil-maps-and-databases/faounesco-soil-map-of-the-world/en/>, 1974.

689 Feraud, G., Giannerini, G., Campredon, R., Stillman, C.J.: Geochronology of some canarian dike swarms:
690 contribution to the volcano-tectonic evolution of the archipelago, *J. Volcanol. Geotherm. Res.*, 25,
691 29–52, [https://doi.org/10.1016/0377-0273\(85\)90003-4](https://doi.org/10.1016/0377-0273(85)90003-4), 1985.

692 Fernández, C., Casillas, R., Ahijado, A., Perelló, V., Hernández-Pacheco, A.: Shear zones as a result of
693 intraplate tectonics in oceanic crust: the example of the Basal Complex of Fuerteventura (Canary
694 Islands), *Jour. Struct. Geol.*, 19, 41–57, [https://doi.org/10.1016/S0191-8141\(96\)00074-0](https://doi.org/10.1016/S0191-8141(96)00074-0), 1997.

695 Frisch, T.: In: Schmincke, H. U., Sumita, M.: Geological evolution of the Canary Islands: a young volcanic
696 archipelago adjacent to the old African continent, *Bull Volcanol.*, 74, 1255–1256,
697 <https://doi.org/10.1007/s00445-012-0605-1>, 2012.

698 Fúster, J. M., Cendrero, A., Gastesi, P., Ibarrola, E., López-Ruiz, J.: Geología y volcanología de las Islas
699 Canarias- Fuerteventura, Instituto “Lucas Mallada”, Consejo Superior de Investigaciones Científicas,
700 Madrid. 239 pp, 1968.

701 Goodenough, K. M., Schilling, J., Jonsson, E., Kalvig, P., Charles, N., Tuduri, J., Deady, E. A., Sadeghi,
702 M., Schiellerup, H., Müller, A., Bertrand, G., Arvanitidis, N., Eliopoulos, D. G., Shaw, R. A., Thrane,
703 K., Keulen, N.: Europe’s rare earth element resource potential: An overview of REE metallogenetic
704 provinces and their geodynamic setting, *Ore Geol. Rev.*, 72, 838–856,
705 <https://doi.org/10.1016/j.oregeorev.2015.09.019>, 2016.

706 Goudie, A. S., Middleton, N. J.: Saharan dust storms: nature and consequences, *Earth Sci. Rev.*, 56, 179–
707 204, [https://doi.org/10.1016/S0012-8252\(01\)00067-8](https://doi.org/10.1016/S0012-8252(01)00067-8), 2001.

708 Graedel, T. E., Harper, E. M., Nassar, N. T., Reck, B. K.: Criticality of metals and metalloids, Proceedings
709 of the National Academy of Sciences, 112 4257–4262, <https://doi.org/10.1073/pnas.1500415112>,
710 2015.

711 Gutiérrez, M., Casillas, R., Fernández, C., Balogh, K., Ahijado, A., Castillo, C., Colmenero, J. R., García-
712 Navarro, E.: The submarine volcanic succession of the basal complex of Fuerteventura, Canary
713 Islands: A model of submarine growth and emergence of tectonic volcanic islands, Bulletin of the
714 Geological Society of America, 118, 785–804, <https://doi.org/10.1130/B25821.1>, 2006.

715 Gutiérrez-Elorza, M., Lucha, P., Gracia, F. J., Desir, G., Marín, C., Petit-Maire, N.: Palaeoclimatic
716 considerations of talus flatirons and aeolian deposits in Northern Fuerteventura volcanic island
717 (Canary Islands, Spain), Geomorphology, 197, 1–9, <https://doi.org/10.1016/j.geomorph.2011.09.020>,
718 2013.

719 Haxel, G. B.: Ultrapotassic mafic dikes and rare earth element- and barium-rich carbonatite at Mountain
720 Pass, Mojave Desert, southern California: summary and field trip localities, U.S. Geol. Surv. Open-
721 File Rep., 1219. <http://pubs.usgs.gov/of/2005/1219/>, 2005.

722 Hobson, A., Bussy, F., Hernández, J.: Shallow-level migmatization of gabbros in a metamorphic contact
723 aureole, Fuerteventura Basal Complex, Canary Islands, Journal of Petrology, 39, 1025–1037,
724 <https://doi.org/10.1093/petroj/39.5.1025>, 1998.

725 Hoernle, K., Tilton, G., Le Bas, M.J., Duggen, S., Garbe-Schönberg, D., Geochemistry of oceanic
726 carbonatites compared with continental carbonatites: Mantle recycling of oceanic crustal carbonate,
727 Contrib. Mineral. Petrol., 142, 520–542, <https://doi.org/10.1007/s004100100308>, 2002.

728 Holloway, M. I., Bussy, F.: Trace element distribution among rock-forming minerals from metamorphosed
729 to partially molten basic igneous rocks in a contact aureole (Fuerteventura, Canaries), Lithos, 102,
730 616–639, <https://doi.org/10.1016/j.lithos.2007.07.026>, 2008.

731 Huerta, P., Rodríguez-Berriguete, A., Martín-García, R., Martín-Pérez, A., La-Iglesia-Fernández, A.,
732 Alonso-Zarza, A.: The role of climate and eolian dust input in calcrete formation in volcanic islands
733 (Lanzarote and Fuerteventura, Spain), Palaeogeogr. Palaeoclimatol. Palaeoecol., 417, 66–79,
734 <https://doi.org/10.1016/j.palaeo.2014.10.008>, 2015.

735 Humphreys-Williams, E.R., Zahirovic, S.: Carbonatites and Global Tectonics, Elements, 17, 339–344,
736 <https://doi.org/10.2138/gselements.17.5.339>, 2021.

737 Jahn, R., Blume, H. P., Asio, V. B., Spaargaren, O., Schad, P.: Guidelines for soil description, FAO, Rome
738 97 p, <https://www.fao.org/3/a0541e/a0541e.pdf>, 2006.

739 Jyothi, R. K., Thenepalli, T., Ahn, J. W., Parhi, P. K., Chung, K. W., Lee, J. Y.: Review of rare earth
740 elements recovery from secondary resources for clean energy technologies: grand opportunities to
741 create wealth from waste, J. Clean. Prod., 267, 122048, <https://doi.org/10.1016/j.jclepro.2020.122048>,
742 2020.

743 Kamenetsky, V.S., Doroshkevich, A.G., Elliot, H.A.L., Zaitsev, A.N., Carbonatites: Contrasting, Complex,
744 and Controversial, Elements, 17, 307–314, <https://doi.org/10.2138/gselements.17.5.307>, 2021.

745 Kravchenko, S. M., Pokrovsky, B. G.: The Tomtor alkaline ultrabasic massif and related REE-Nb deposits,
746 northern Siberia, Economic Geology, 90, 676–689, <https://doi.org/10.2113/gsecongeo.90.3.676>,
747 1995.

- 748 Kravchenko, S. M., Czamanske, G., Fedorenko, V. A.: Geochemistry of carbonatites of the Tomtor massif,
749 *Geochem. Int.*, 41, 545–558, ISSN: 0016-7029, 2003.
- 750 Lai, X., Yang, X., Santosh, M., Liu, Y., Ling, M.: New data of the Bayan Obo Fe-REE-Nb deposit, Inner
751 Mongolia: Implications for ore genesis, *Precambrian Research*, 263, 108–122,
752 <https://doi.org/10.1016/j.precamres.2015.03.013>, 2015.
- 753 Le Bas, M. J.: The pyroxenite-ijolite-carbonatite intrusive igneous complexes of Fuerteventura, Canary
754 Islands, *J. Geol. Soc. London*, 138, 496, <https://doi.org/10.1144/gsjgs.138.4.0493>, 1981.
- 755 Le Bas, M. J., Rex, D. C., Stillman, C. J.: The early magmatic chronology of Fuerteventura, *Geol. Mag.*,
756 123, 287–298, <https://doi.org/10.1017/S0016756800034762>, 1986.
- 757 Le Maitre, R. W., *Igneous Rocks: a Classification and Glossary of Terms*, Cambridge University Press,
758 Cambridge, U.K., 2002.
- 759 Le Maitre, R. W., Streckeisen, A., Zanettin, B., Le Bas, M. J., Bonin, B., Bateman, P., Bellieni, G., Dudek,
760 A., Efremova, S., Keller, J., Lameyre, J., Sabine, P. A., Schmid, R., Sorensen, H., Woolley, A. R.:
761 *Igneous Rocks: A Classification and Glossary of Terms*, 2nd Edition, Cambridge, UK, Cambridge
762 Univ. Press, ISBN: 9780521619486, 2005.
- 763 Liu, Y. L., Ling, M. X., Williams, I. S., Yang, X. Y., Wang, C. Y., Sun, W.: The formation of the giant
764 Bayan Obo REE-Nb-Fe deposit, North China, Mesoproterozoic carbonatite overprinted Paleozoic
765 dolomitization, *Ore Geology Reviews*, 92, 73–83, <https://doi.org/10.1016/j.oregeorev.2017.11.011>,
766 2018.
- 767 Long, K. R., Van Gosen, B. S., Foley, N. K., Cordier, D.: The principal rare earth elements deposits of the
768 United States: A summary of domestic deposits and a global perspective,
769 <https://pubs.usgs.gov/sir/2010/5220/>, 2010.
- 770 Longpré, M. A., Felpeto, A.: Historical volcanism in the Canary Islands; part 1: A review of precursory
771 and eruptive activity, eruption parameter estimates, and implications for hazard assessment, *Journal*
772 *of Volcanology and Geothermal Research*, 419, 107363,
773 <https://doi.org/10.1016/j.jvolgeores.2021.107363>, 2021.
- 774 Machado-Yanes, M. C.: Reconstrucción paleoecológica y etnoarqueológica por medio del análisis
775 antracológico. La Cueva de Villaverde, Fuerteventura, In: *Biogeografía Pleistocena-Holocena de la*
776 *Península Ibérica*, 261274, Ramil-Rego, P., Fernández-Rodríguez, C., Rodríguez-Guitián, M. (Eds.),
777 ISBN 84-453-1716-4, 261 p, 1996.
- 778 Mangas, J., Pérez-Torrado, F. J., Reguillón, R. M., Cabrera, M. C.: Prospección radiométrica en rocas
779 alcalinas y carbonatitas de la serie plutónica I de Fuerteventura (Islas Canarias). Resultados
780 preliminares e implicaciones metalogénicas, *Actas del III Congreso Geológico de España y VIII*
781 *Congreso Latinoamericano de Geología*. Salamanca, 3, 389–393, ISBN: 84-600-8114-1, 1992.
- 782 Mangas, J., Pérez-Torrado, F. J., Reguillón, R. M., Martín-Izard, A.: Mineralizaciones de tierras raras
783 ligadas a los complejos intrusivos alcalino-carbonatíticos de Fuerteventura (Islas Canarias), *Bol. Soc.*
784 *Esp. Min.*, 17, 212–213, 1994.
- 785 Mangas, J., Pérez-Torrado, F. J., Reguillón, R. M., Martín-Izard, A.: Rare earth minerals in carbonatites of
786 Basal Complex of Fuerteventura (Canary Islands, Spain), In: *Mineral Deposit: Research and*

787 Exploration, where do they meet? Ed. Balkema, Rotterdam, 475–478, ISBN-13: 978-9054108894,
788 1997.

789 Mariano, A. N., Mariano, Jr. A.: Rare earth mining and exploration in North America, *Elements*, 8, 369–
790 376, <https://doi.org/10.2113/gselements.8.5.369>, 2012.

791 Massari, S., Ruberti, M.: Rare earth elements as critical raw materials: Focus on international markets and
792 future strategies, *Resour. Policy*, 38, 36–43, <https://doi.org/10.1016/j.resourpol.2012.07.001>, 2013.

793 McDonough, W., Sun, W.: The composition of the Earth, *Chemical Geology*, 67, 1050–1056,
794 [https://doi.org/10.1016/0009-2541\(94\)00140-4](https://doi.org/10.1016/0009-2541(94)00140-4), 1995.

795 Méndez-Ramos, J., Acosta-Mora, P., Ruiz-Morales, J. C., Hernández, T., Morge, M. E., Esparza, P.:
796 Turning into the blue: materials for enhancing TiO₂ photocatalysis by up-conversion photonics, *RSC*
797 *Advances*, 3, 23028–23034, <https://doi.org/10.1039/C3RA44342F>, 2013.

798 Menéndez, I., Díaz-Hernández, J. L., Mangas, J., Alonso, I., Sánchez-Soto, P. J.: Airborne dust
799 accumulation and soil development in the North-East sector of Gran Canaria (Canary Islands, Spain),
800 *J. Arid Environ.*, 71, 57–81, <https://doi.org/10.1016/j.jaridenv.2007.03.011>, 2007.

801 Menéndez, I., Campeny, M., Quevedo-González, L., Mangas, J., Llovet, X., Tauler, E., Barrón, V., Torrent,
802 J., Méndez-Ramos, J.: Distribution of REE-bearing minerals in felsic magmatic rocks and paleosols
803 from Gran Canaria, Spain: Intraplate oceanic islands as a new example of potential, non-conventional
804 sources of rare-earth elements, *Journal of Geochemical Exploration*, 204, 270–288,
805 <https://doi.org/10.1016/j.gexplo.2019.06.007>, 2019.

806 Moore, M., Chakhmouradian, A., Mariano, A. N., Sidhu, R.: Evolution of Rare-earth Mineralization in the
807 Bear Lodge Carbonatite, In: *Ore Geology Reviews*, 64, Mineralogical and Isotopic Evidence,
808 Wyoming, 499, 521, <http://dx.doi.org/10.1016/j.oregeorev.2014.03.015>, 2015.

809 Mourão, C., Mata, J., Doucelance, R., Madeira, J., da Silveira, A.B., Silva, L.C., Moreira, M., Quaternary
810 extrusive calciocarbonatite volcanism on Brava Island (Cape Verde): A nephelinite-carbonatite
811 immiscibility product, *Journal of African Earth Sciences*, 56, 59–74,
812 <https://doi.org/10.1016/j.jafrearsci.2009.06.003>, 2010.

813 Muñoz, M.: Ring complexes of Pájara in Fuerteventura Island, *Bulletin Volcanologique*, 33, 840–861,
814 <https://doi.org/10.1007/BF02596753>, 1969.

815 Muñoz, M., Sagredo, J., de Ignacio, C., Fernández-Suárez, J., Jeffries, T. E.: New data (U-Pb, K-Ar) on the
816 geochronology of the alkaline-carbonatitic association of Fuerteventura, Canary Islands, Spain,
817 *Lithos*, 85, 140–153, <https://doi.org/10.1016/j.lithos.2005.03.024>, 2005.

818 Olson, J.C., Shawe, D. R., Pray, L.C., Sharp, W. N.: Rare-Earth Mineral Deposits of the Mountain Pass
819 District, San Bernardino County, California, *Science*, 119, 325–326,
820 <https://doi.org/10.1126/science.119.3088.325>, 1954.

821 Park, J., Rye, D.M., Broader Impacts of the Metasomatic Underplating Hypothesis, *Geochem. Geophys.*
822 *Geosyst.*, 20, 4180–4829, <https://doi.org/10.1029/2019GC008493>, 2019.

823 Pérez-Torrado, F. J., Carracedo, J. C., Guillou, H., Rodríguez-González, A., Fernández-Turiel, J. L.: Age,
824 duration, and spatial distribution of ocean shields and rejuvenated volcanism: Fuerteventura and
825 Lanzarote, Eastern Canaries, *Journal of the Geological Society of London*, 180,
826 <https://doi.org/10.1144/jgs2022-112>, 2023.

827 Pirajno, F., Yu, H.C.: The carbonatite story once more and associated REE mineral systems, *Gondwana*
828 *Research*, 107, 281–295. <https://doi.org/10.1016/j.gr.2022.03.006>, 2022.

829 Reinhardt, N., Proenza, J., Villanova-de-Benavent, C., Aiglsperger, T., Bover-Arnal, T., Torró, L., Salas,
830 R., Dziggel, A.: Geochemistry and Mineralogy of Rare Earth Elements (REE) in Bauxitic Ores of the
831 Catalan Coastal Range, NE Spain, *Minerals*, 8, 562, <https://doi.org/10.3390/min8120562>, 2018.

832 Rudnick, R.L., Gao, S.: Composition of the Continental Crust, In: Holland, H.H., Turekian, K.K. (editors):
833 *Treatise on Geochemistry*, 4, 1–51, <https://doi.org/10.1016/B978-0-08-095975-7.00301-6>, 2014.

834 Scheuvens, D., Schütz, L., Kandler, K., Ebert, M., Weinbruch, S.: Bulk composition of northern African
835 dust and its source sediments—a compilation, *Earth Sci. Rev.*, 116, 170–194,
836 <https://doi.org/10.1016/j.earscirev.2012.08.005>, 2013.

837 Schmincke, H., Sumita, M.: Geological evolution of the Canary Islands: a young volcanic archipelago adjacent
838 to the old African Continent, Ed. Görres, Koblenz, 200 p, ISBN: 978-3-86972-005-0, 2010.

839 Smith, M. P., Campbell, L. S., Kynicky, J.: A review of the genesis of the world class Bayan Obo Fe-REE-Nb
840 deposits, Inner Mongolia, China: multistage processes and outstanding questions, *Ore Geology Reviews*,
841 64, 459–476, <https://doi.org/10.1016/j.oregeorev.2014.03.007>, 2015.

842 Smith, M. P., Moore, K., Kavecsánszki, D., Finch, A. A., Kynicky, J., Wall, F.: From mantle to critical zone:
843 A review of large and giant-sized deposits of the rare earth elements, *Geoscience Frontiers*, 7, 315–334,
844 <https://doi.org/10.1016/j.gsf.2015.12.006>, 2016.

845 Steiner, C., Hobson, A., Favre, P., Stampfli, G. M.: Early Jurassic sea-floor spreading in the central Atlantic
846 — the Jurassic sequence of Fuerteventura (Canary Islands), *Geological Society of American Bulletin*,
847 110, 1304–1317, [https://doi.org/10.1130/0016-7606\(1998\)110<1304:MSOFCI>2.3.CO;2](https://doi.org/10.1130/0016-7606(1998)110<1304:MSOFCI>2.3.CO;2), 1998.

848 Torró, L., Proenza, J. A., Aiglsperger, T., Bover-Arnal, T., Villanova-de-Benavent, C., Rodríguez-García,
849 D., Ramírez, A., Rodríguez, J., Mosquea, L.A., Salas, R.: Geological, geochemical and mineralogical
850 characteristics of REE-bearing Las Mercedes bauxite deposit, Dominican Republic, *Ore Geol. Rev.*,
851 89, 114–131, <https://doi.org/10.1016/j.oregeorev.2017.06.017>, 2017.

852 Torró, L., Villanova, C., Castillo, M., Campeny, M., Gonçalves, A. O., Melgarejo, J. C.: Niobium and rare
853 earth minerals from the Virulundo carbonatite, Namibe, Angola, *Mineralogical Magazine*, 76, 393–
854 409, <https://doi.org/10.1180/minmag.2012.076.2.08>, 2012.

855 Troll, V., Carracedo, J. C.: The Geology of Fuerteventura, In: Troll, V., Carracedo, J. C., Weismaier, S.
856 (eds), *The Geology of Canary Islands*, Elsevier, 531–582. [http://dx.doi.org/10.1016/B978-0-12-](http://dx.doi.org/10.1016/B978-0-12-809663-5.00008-6)
857 [809663-5.00008-6](http://dx.doi.org/10.1016/B978-0-12-809663-5.00008-6), 2016.

858 van den Bogaard, P.: The origin of the Canary Island Seamount Province - New ages of old seamounts,
859 *Scientific Reports*, 3, 2107. <https://doi.org/10.1038/srep02107>, 2013.

860 Wang, Q., Deng, J., Liu, X., Zhang, Q., Sun, S., Jiang, C., Zhou, F.: Discovery of the REE minerals and its
861 geological significance in the Quyang bauxite deposit, West Guangxi, China, *J. Asian Earth Sci.*, 39,
862 701–712, <https://doi.org/10.1016/j.jseaes.2010.05.005>, 2010.

863 Wang, X., Jiao, Y., Du, Y., Ling, W., Wu, L., Cui, T., Zhou, Q., Jin, Z., Lei, Z., Wen, S.: REE mobility
864 and Ce anomaly in bauxite deposit of WZD area, Northern Guizhou, China, *J. Geochem Explor.*, 133,
865 103–117, <https://doi.org/10.1016/j.gexplo.2013.08.009>, 2013.

866 Wang, Z.Y., Fan, H.R., Zhou, L., Yang, K.F., She, H.D., Carbonatite-related REE deposits: An
867 overview, *Minerals*, 10, 965. <https://doi.org/10.3390/min10110965>, 2020.

868 Warr, L. N.: IMA–CNMNC approved mineral symbols, *Mineralogical Magazine*, 85, 291–
869 320, <https://doi.org/10.1180/mgm.2021.43>, 2021.

870 Weidendorfer, D., Schmidt, M.W., Mattsson, H.B.: Fractional crystallization of Si-undersaturated alkaline
871 magmas leading to unmixing of carbonatites on Brava Island (Cape Verde) and a general model of
872 carbonatite genesis in alkaline magma suites, *Contributions to Mineralogy and Petrology*, 171, 43,
873 <https://doi.org/10.1007/s00410-016-1249-5>, 2016.

874 Wondraczek, L., Tyystjärvi, E., Méndez-Ramos, J., Müller, F. A., Zhang, Q.: Shifting the Sun: Solar
875 Spectral Conversion and Extrinsic Sensitization in Natural and Artificial Photosynthesis, *Advanced*
876 *Science*, 2, 1500218, <https://doi.org/10.1002/advs.201500218>, 2015.

877 Woolley, A.R., Kjarsgaard, B.A. (2008): Carbonatites of the world: map and database. *Mineralogical*
878 *Magazine* 71, 718.

879 Wu, C.: Bayan Obo Controversy: Carbonatites versus Iron Oxide-Cu-Au-(REE-U), *Resource Geology*, 58,
880 348–354, <https://doi.org/10.1111/j.1751-3928.2008.00069.x>, 2008.

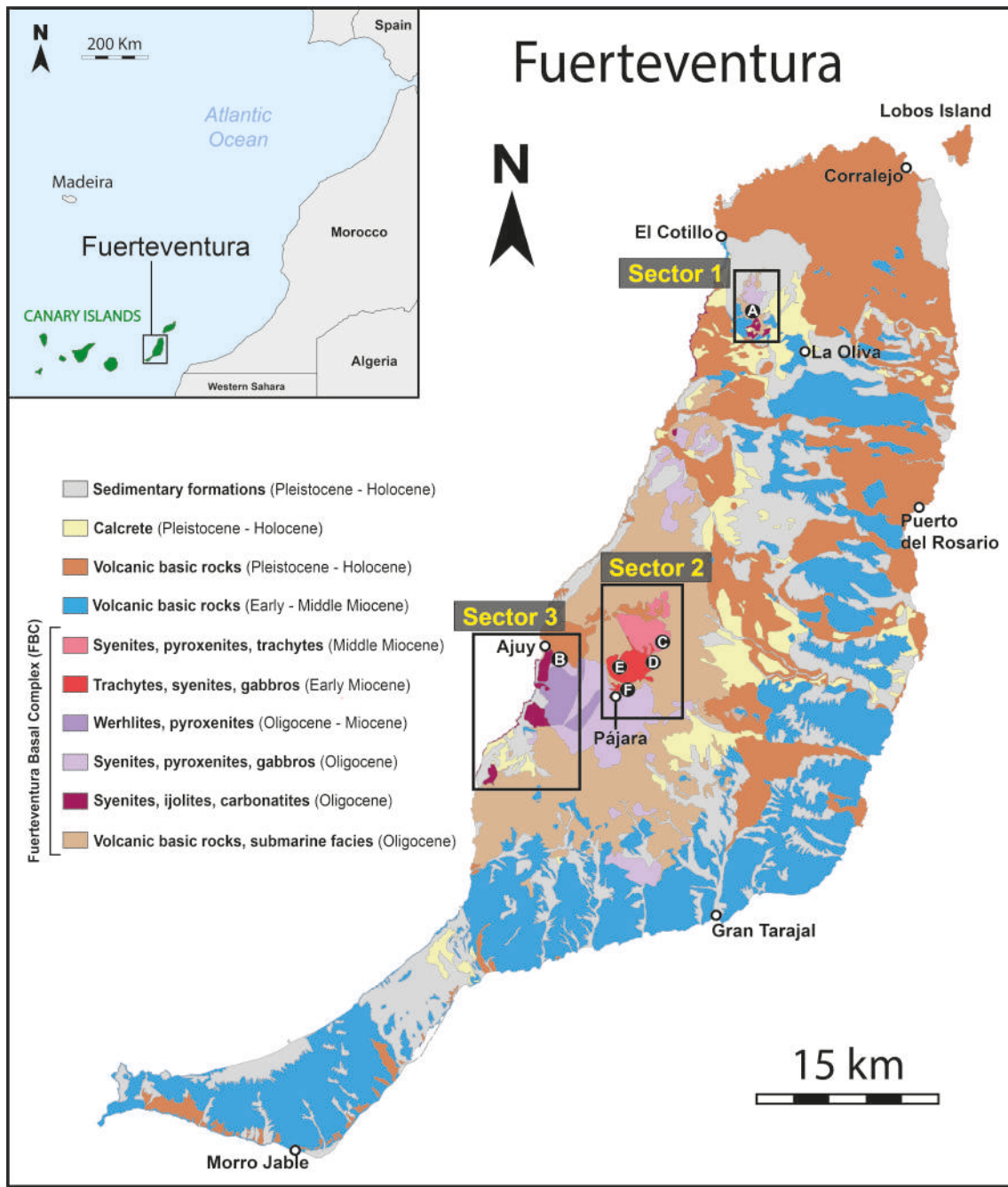
881 Yang, K., Fan, H., Pirajno, F., Li, X.: The bayan Obo (China) giant REE accumulation conundrum
882 elucidated by intense magmatic differentiation of carbonatite, *Geology*, 47, 1198–1202,
883 <https://doi.org/10.1130/G46674.1>, 2019.

884 Yaxley, G.M., Anenburg, M., Tappe, S., Decree, S., Guzmics, T.: Carbonatites: Classification, Sources,
885 Evolution, and Emplacement, *Annual Reviews on Earth and Planetary Sciences*, 50, 261–293,
886 <https://doi.org/10.1146/annurev-earth-032320-104243>, 2022.

887 Zazo, C., Goy, J. L., Hillaire-Marcel, C., Gillot, P. Y., Soler, V., González, J. A., Dabrio, C. J., Ghaleb, B.:
888 Raised marine sequences of Lanzarote and Fuerteventura revisited –a reappraisal of relative sea-level
889 changes and vertical movements in the eastern Canary Islands during the Quaternary, *Quaternary*
890 *Science Reviews*, 21, 2019–2046, [https://doi.org/10.1016/S0277-3791\(02\)00009-4](https://doi.org/10.1016/S0277-3791(02)00009-4), 2002.

891 Zhukova, I. A., Stepanov, A. S., Jiang, S. Y., Murphy, D., Mavrogenes, J., Allen, C., Chen, W., Bottrill,
892 R.: Complex REE systematics of carbonatites and weathering products from uniquely rich Mount
893 Weld REE deposit, Western Australia, *Ore Geology Reviews*, 139, 104539,
894 <https://doi.org/10.1016/j.oregeorev.2021.104539>, 2021.

895



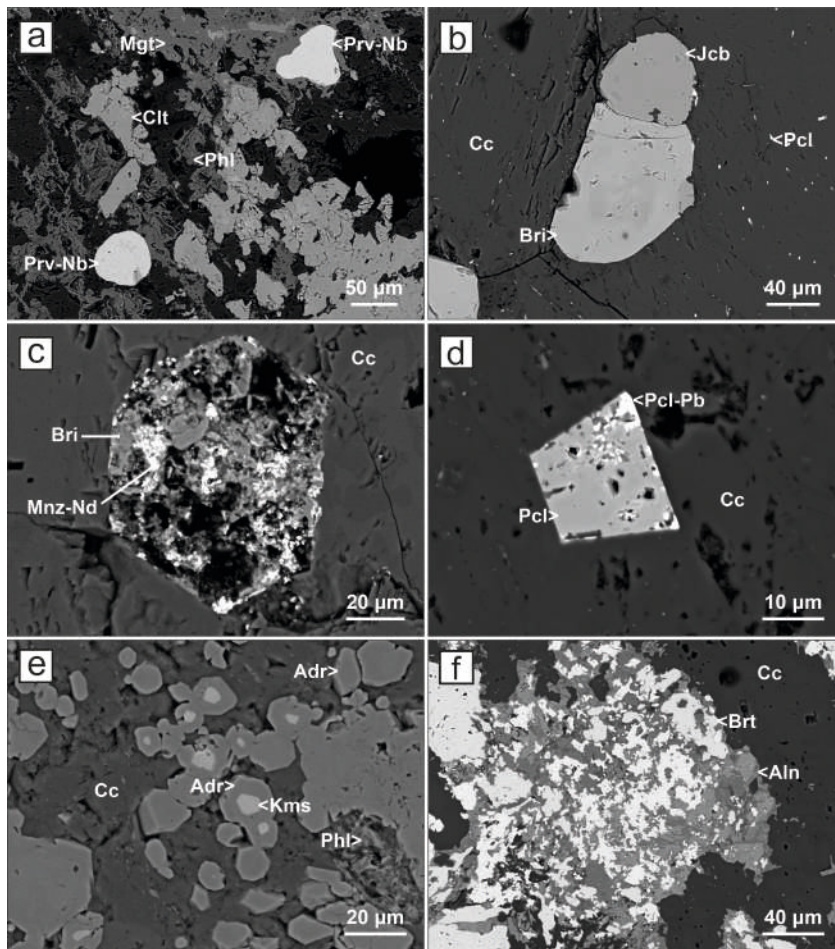
897
 898
 899
 900
 901
 902
 903
 904
 905

Figure 1: Simplified geological map of Fuerteventura Island (modified from Balcells et al., 2006) showing the location of the three study sectors for the assessment of REE content in the FBC. Additionally, the studied weathering profiles are also indicated, as: (A) Agua Salada ravine; (B) Aulagar ravine; (C) Palomares ravine; (D) FV-30 road; (E) Las Peñitas quarry; (F) Pájara.



907

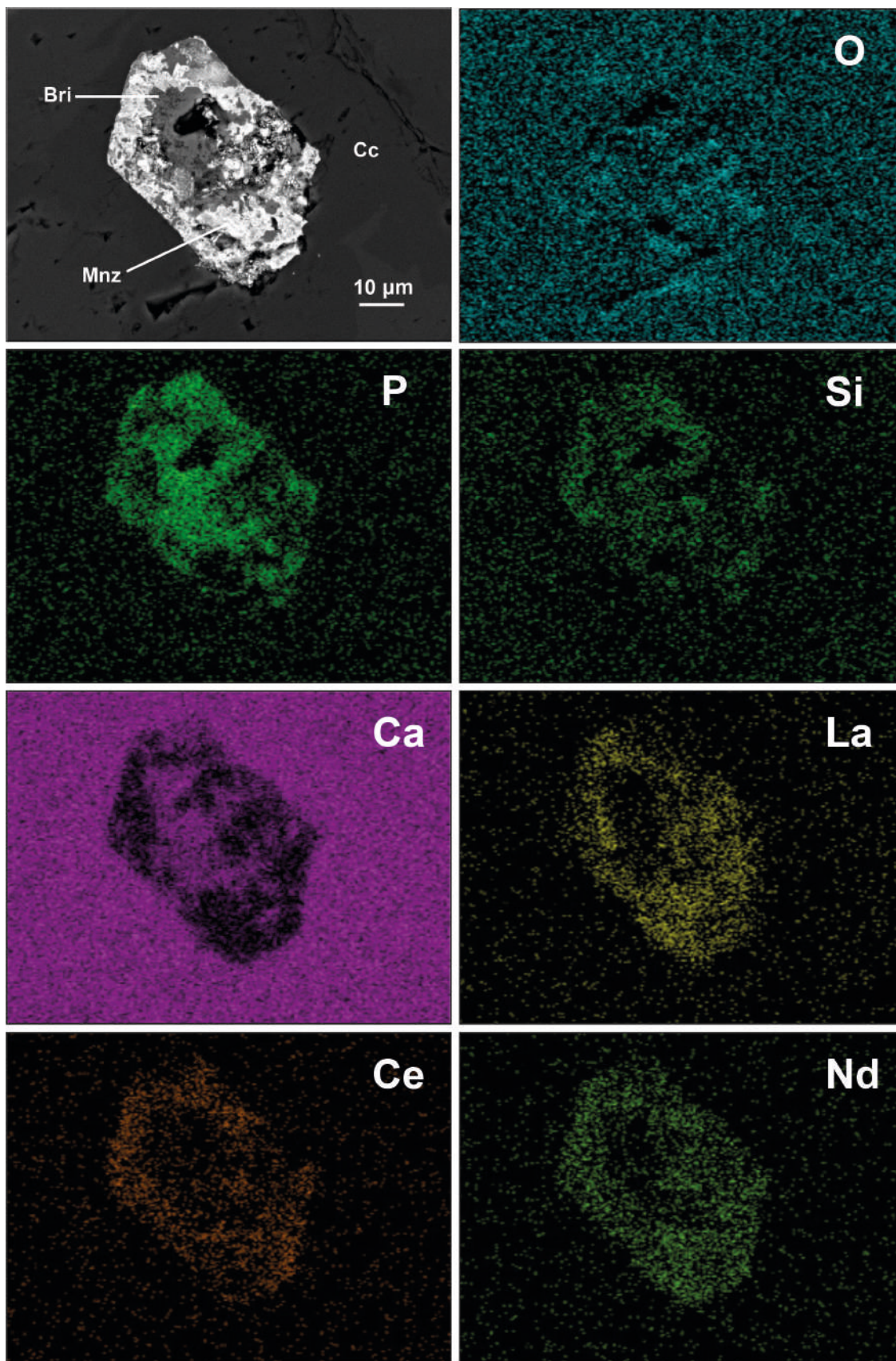
908 **Figure 2:** (a), (b) Images showing typical outcrops of the FBC in the southern area of Ajuy (sector 3;
 909 Figure 1). The images highlight characteristic swarms of alkaline and carbonatitic intrusions (whitish)
 910 intersected by later-intruded basaltic dikes (black colour). (c) Detailed view of a carbonatitic dike located
 911 in a shear zone of sector 3, exhibiting distinct linear sigmoidal structures resulting from deformation. (d)
 912 Detailed view of centimetre-sized phlogopite crystals within a carbonatitic dike outcropping in sector 3,
 913 displaying a typical pegmatitic texture. (e) Overview of an outcrop of metric-scale carbonatitic dikes in the
 914 sector 1 area.



916

917 **Figure 3:** SEM (backscattered electron, BSE) images of the Fuerteventura carbonatites. (a) Subhedral
 918 crystals of niobium-rich perovskite (Prv-Nb) associated with phlogopite (Phl) and magnetite (Mgt)
 919 aggregates. The association has been affected by secondary hydrothermal processes, leading to the
 920 formation of celestine (Clt). (b) Typical subhedral crystal of jacobsite (Jcb) associated with britholite (Bri).
 921 Both crystals are hosted in magmatic calcite (Cc), with numerous disseminated microcrystals of pyrochlore
 922 (Pcl). (c) Partially altered subhedral grain of britholite (Bri) hosted in magmatic calcite (Cc). The alteration
 923 process led to the formation of secondary REE phosphates such as monazite-Nd (Mnz-Nd). (d) Euhedral
 924 crystal of pyrochlore (Pcl) hosted in calcite (Cc). Brighter areas developed on the grain's borders correspond
 925 to plumbopyrochlore (Pcl-Pb) zonation. (e) Typical mineral association related to small skarn like areas
 926 associated with carbonatites. Subhedral zoned crystals of andradite (Adr), hosted in calcite (Cc) and
 927 phlogopite (Phl), with a significant Zr zoning leading to kerimasite (Kms) cores. (f) Typical low-
 928 metamorphic alteration developed on carbonatites composed of allanite (Aln) aggregates hosted in calcite
 929 (Cc) and associated with secondary baryte (Brt). Abbreviations of mineral names in all the pictures follow
 930 the criteria proposed by Warr (2021).

931 **Figure 4**



932

933

934

Figure 4: Wavelength-dispersive X-ray maps of representative compositional elements for an altered grain of britholite (Bri) hosted in calcite (Cc) and partially transformed into secondary monazite (Mnz).

935 **Figure 5**



936

937 **Figure 5: (a)** General view of a typical surface outcrop of Quaternary calcrete located in the Aulagar ravine
938 area (profile B, sector 3; Fig.1). **(b)** Centimetre-thick calcrete layer filling a fracture between two
939 carbonatitic dikes in the Aulagar ravine area (profile B, sector 3; Fig.1). **(c)** Calcrete layer developed within
940 fractures between carbonatitic rocks in the Agua Salada ravine area (profile A, sector 1; Fig.1).

941

942

943

944

945

946

947

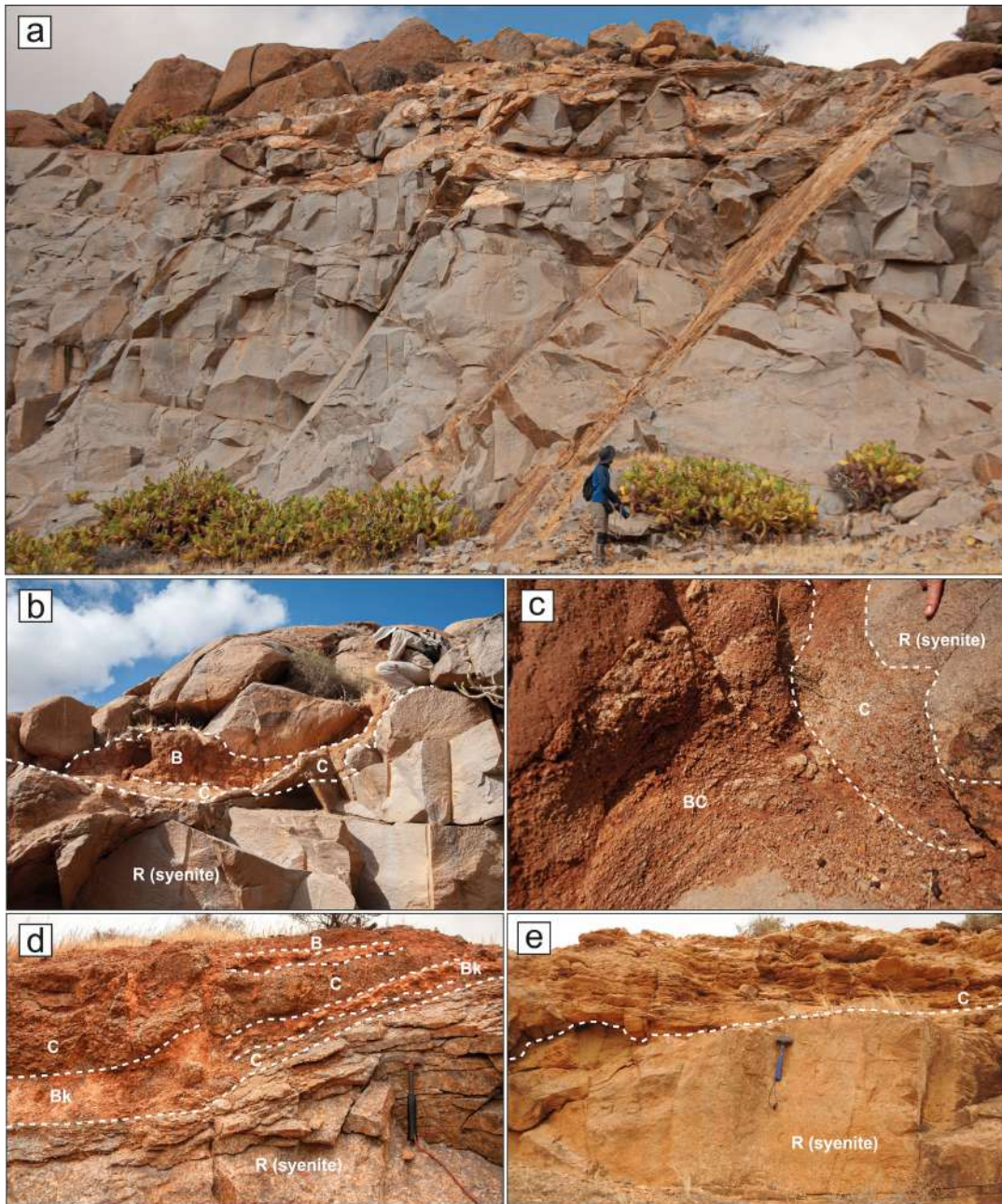
948

949

950

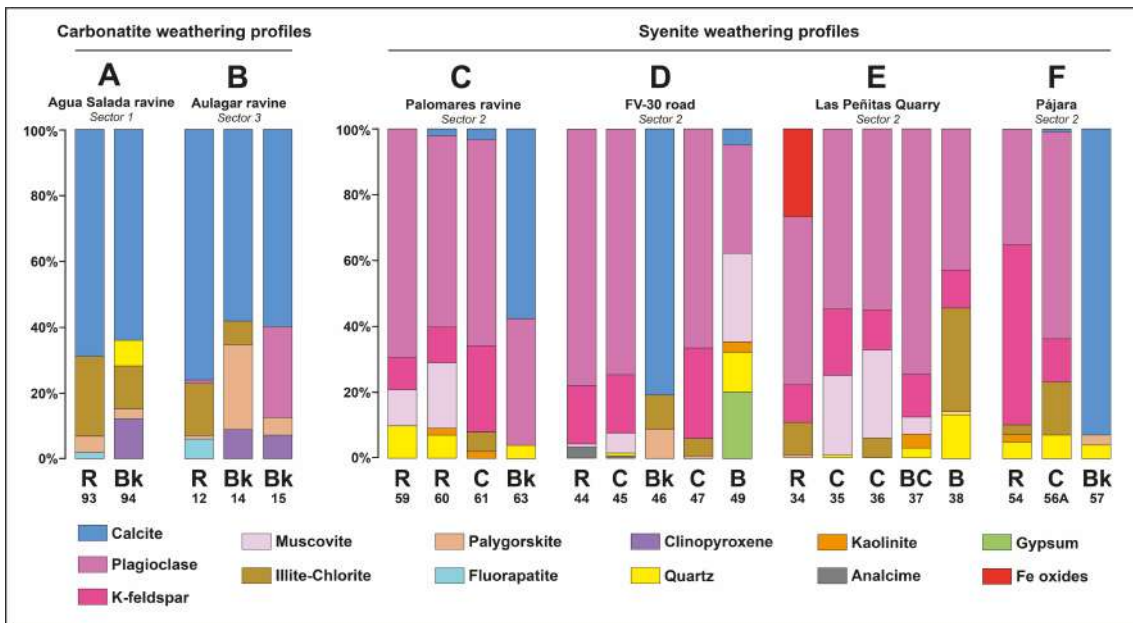
951

952



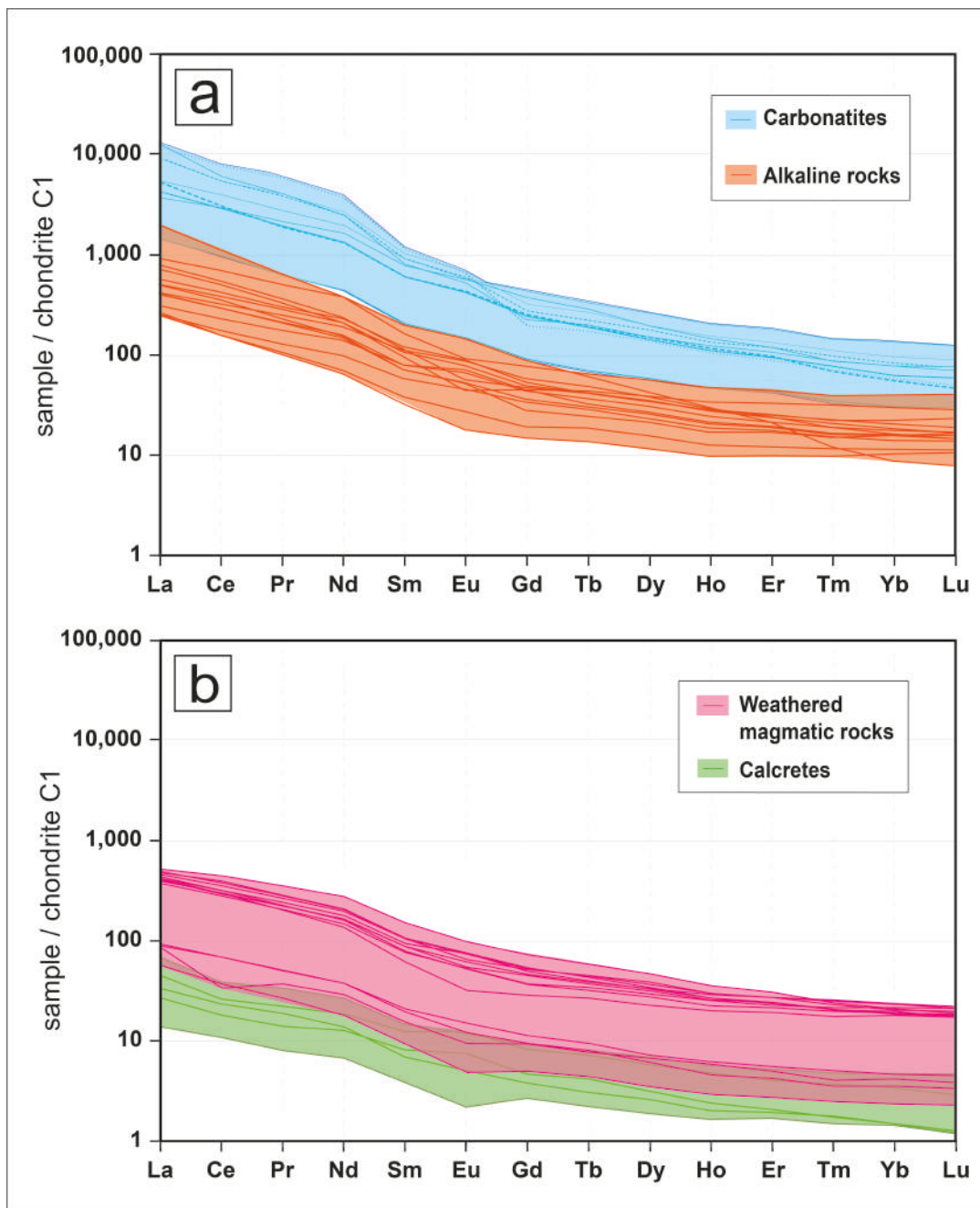
954

955 **Figure 6: (a)** General view of Las Peñitas quarry syenite outcrop (profile E, sector 2; Fig.1) where it is
 956 possible to distinguish different fractures filled by injected secondary weathering products. **(b)** Syenite
 957 weathering profile in Las Peñitas quarry (profile E, sector 2; Figure 1) showing surface erosion and B, BC
 958 and C horizons injected in the syenite bedrock (R). **(c)** Weathering profile displaying the development of
 959 C and BC horizons associated with a syenite protolith (R), located in Las Peñitas quarry (profile E, sector
 960 2; Figure 1). **(d)** Weathering profile developed on syenite in the FV-30 road area (profile D, sector 2),
 961 exhibiting the development of C, B and calcrete (Bk) horizons. **(e)** Weathering profile on syenite protolith
 962 (R) displaying a metric sized C horizon in the Pájara area (profile F, sector 2; Figure 1).



964
 965 **Figure 7:** Graphical mineralogical quantification of the studied weathering profiles: (A) Agua Salada
 966 ravine; (B) Aulagar ravine; (C) Palomares ravine; (D) FV-30 road; (E) Las Peñitas quarry; (F) Pájara. The
 967 corresponding class assigned to the edaphic horizons (B, BC, Bk, C, R) and the sample number are shown
 968 at the foot of the columns.

969
 970
 971
 972
 973
 974
 975
 976
 977
 978
 979
 980
 981
 982
 983
 984



986

987

988 **Figure 8:** REE plots of the studied Fuerteventura lithologies normalised to C1 chondrites. Normalisation

989 values are from McDonough and Sun (1995).

990

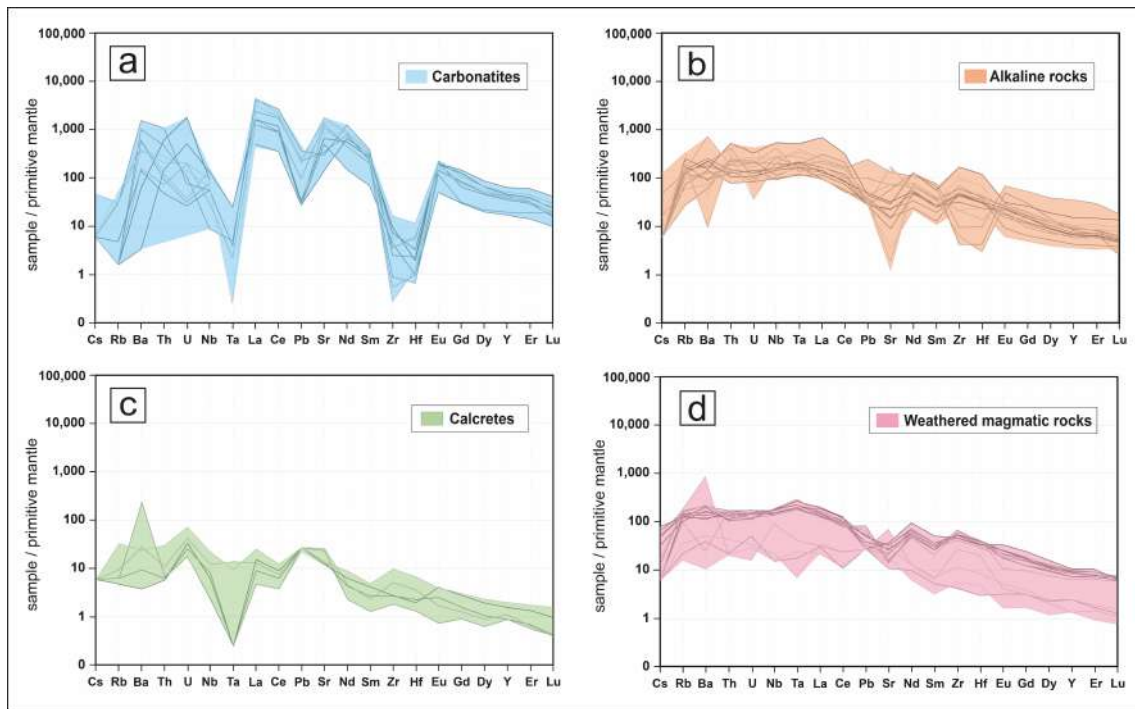
991

992

993

994

995 **Figure 9**



996

997 **Figure 9:** Multi-elemental trace element plots of Fuerteventura intrusive lithologies normalised to the
998 primitive mantle. Normalisation values from McDonough and Sun (1995).

999

1000

1001

1002

1003

1004

1005

1006

1007

1008

1009

1010

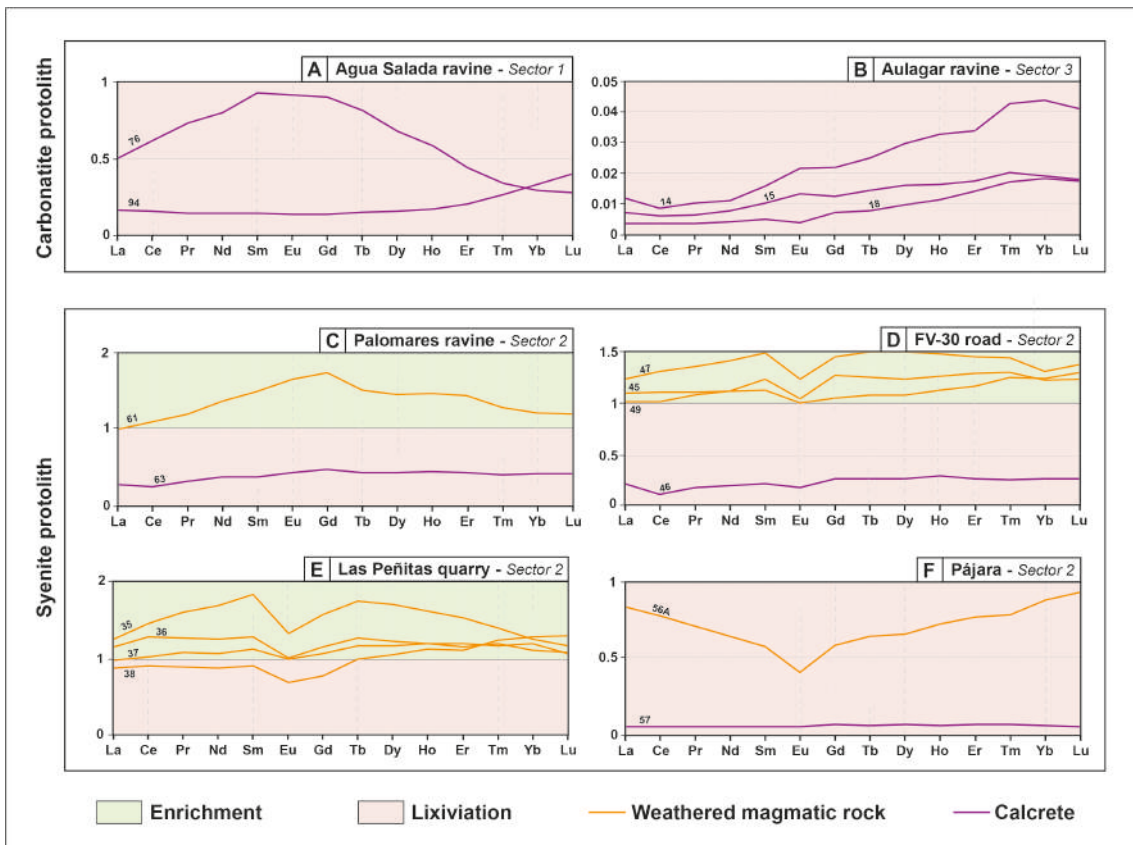
1011

1012

1013

1014

1015 **Figure 10**



1016

1017 **Figure 10:** REE weathering enrichment/leaching diagrams between primary magmatic protoliths
1018 (carbonatites and syenites) and the associated weathering products from the studied profiles (Figure 1). The
1019 sample number is labelled on the corresponding pattern line.

1020

1021

1022

1023

1024

1025

1026

1027

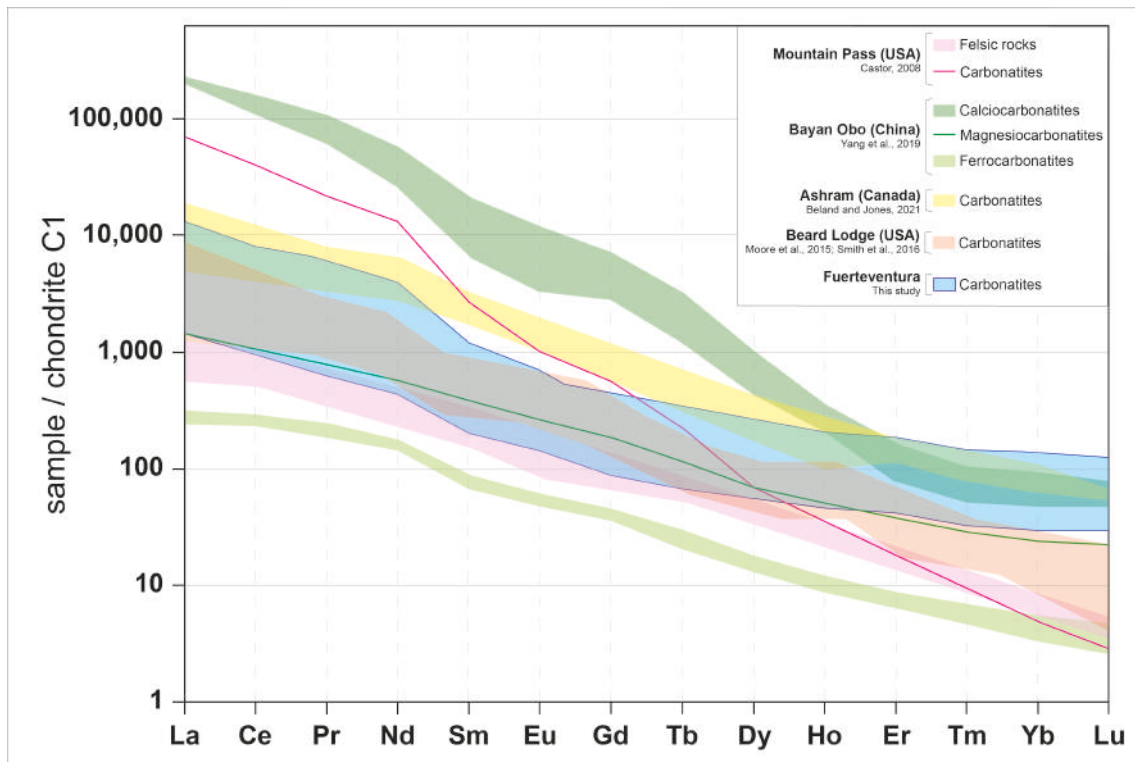
1028

1029

1030

1031

1032 **Figure 11**



1033

1034 **Figure 11:** REE plot of the studied Fuerteventura carbonatites compared to other carbonatitic localities
 1035 worldwide where REE deposits have been reported. REE contents for comparison are from Castor (2008),
 1036 Yang et al. (2019), and Beland and Jones (2021). Normalisation values are from McDonough and Sun
 1037 (1995).

1038